Contrib Mineral Petrol (2007) 154:385–408
DOI 10.1007/s00410-007-0199-3

ORIGINAL PAPER

~3,850 Ma tonalites in the Nuuk region, Greenland: geochemistry and their reworking within an Eoarchaean gneiss complex

Allen P. Nutman · Vickie C. Bennett · Clark R. L. Friend · Kenji Horie · Hiroshi Hidaka

Received: 27 February 2006 / Accepted: 27 March 2007 / Published online: 12 July 2007

Abstract The Eoarchaean (>3,600 Ma) Itsaq Gneiss Complex of southern West Greenland is dominated by polyphase orthogneisses with a complex Archaean tectonothermal history. Some of the orthogneisses have c. 3,850 Ma zircons, and they vary from rare single phase metatonalites to more common complexly banded migmatites. This is due to heterogeneous strain, in situ anatexis and granitic veining superimposed during younger tectonothermal events. In the single-phase tonalites with c. 3,850 Ma zircon, oscillatory-zoned prismatic zircon is all 3,850 Ma old, but shows patchy ancient loss of radiogenic Pb. SHRIMP spot analyses and laser ablation ICP-MS depth profiling show that thin (usually < 10 μm) younger (3,660–3,590 Ma and Neoarchaean) shells of lower Th/U metamorphic zircon are present on these 3,850 Ma zircons. Several samples with this simple zircon population occur on islands near Akilia. In contrast, migmatites usually contain more complex zircon populations, with often more than one generation of igneous zircon present. Additional zircon dating of banded gneisses across the Complex shows that samples with c. 3,850 Ma igneous zircon are not just a phenomenon restricted to Akilia and adjacent islands. For example, migmatites from Itilleq (c. 65 km from Akilia) contain variable amounts of oscillatory-zoned 3,850 Ma and 3,650 Ma zircon, interpreted, respectively, as the rock age and the time of crustal melting under Eoarchaean metamorphism. With only 110–140 ppm Zr in the tonalites and likely magmatic temperatures of >850°C, zircon solubility–melt composition relationships show that they were only one-third saturated in zircon. Any zircon entrained in the precursor magmas would thus have been highly soluble. Combined with the cathodoluminesence imaging, this demonstrates that the c. 3,850 Ma oscillatory zoned zircon crystallised out of the melt and hence gives a magmatic age. Thus the rare well-preserved tonalites and palaeosome in migmatites testify that c. 3,850 Ma quartzo–feldspathic rocks are a widespread (but probably minor) component in the Itsaq Gneiss Complex. C. 3,850 Ma zircon with negative Eu anomalies (showing growth in felsic systems) also occurs as detrital grains in rare c. 3,800 Ma metaquartzites and as inherited grains in some 3,660 Ma granites (*sensu stricto*). These demonstrate that still more c. 3,850 Ma rocks were present, but were recycled into Eoar-

Communicated by I. Parsons.

Electronic supplementary material The online version of this article (doi:10.1007/s00410-007-0199-3) contains supplementary material, which is available to authorized users.

A. P. Nutman · V. C. Bennett
Research School of Earth Sciences, Australian National University, Canberra, ACT 0200, Australia

A. P. Nutman
Department of Earth and Marine Science, Australian National University, Canberra, ACT 0200, Australia

A. P. Nutman (✉)
Beijing SHRIMP Centre, Institute of Geology, Chinese Academy of Geological Sciences, 26 Baiwanzhuang Road, Beijing 100037, People's Republic of China
e-mail: nutman@bjshrimp.cn

C. R. L. Friend
45 Stanway Road, Headington, Oxford OX3 0BP, UK

K. Horie
Department of Earth and Planetary Systems Sciences, University of Hiroshima, 1-3-1 Kagamiyama, Higashi-Hiroshima 739-8526, Japan

K. Horie · H. Hidaka
Department of Science and Engineering, The National Science Museum, 3-23-1, Hyakunin-cho, Shinjuku-ku, Tokyo 169-0073, Japan

chaean sediments and crustally derived granites. The major and trace element characteristics (e.g. LREE enrichment, HREE depletion, low MgO) of the best-preserved c. 3,850 Ma rocks are typical of Archaean TTG suites, and thus argue for crust formation processes involving important contributions from melting of hydrated mafic crust to the earliest Archaean. Five c. 3,850 Ma tonalites were selected as the best preserved on the basis of field criteria and zircon petrology. Four of these samples have overlapping initial ε_{Nd} (3,850 Ma) values from +2.9 to +3.6± 0.5, with the fourth having a slightly lower value of +0.6. These data provide additional evidence for a markedly LREE-depleted early terrestrial mantle reservoir. The role of c. 3,850 Ma crust should be considered in interpreting isotope signatures of the younger (3,800–3,600 Ma) rocks of the Itsaq Gneiss Complex.

Keywords Eoarchaean · Tonalites · Crustal evolution · Zircons · Greenland · Nd isotopes · Itsaq Gneiss Complex

Introduction

Eoarchaean rocks (>3,600 Ma) provide a geochemical window onto the early Earth. These rocks are predominantly tonalitic–granitic ‘‘banded grey gneisses‘‘ derived from plutonic protoliths, that enclose remnants of ultramafic, gabbroic and supracrustal rocks (e.g., McGregor 1973, 1979; Bridgwater et al. 1976; Collerson and Bridgwater 1979; Black et al. 1986; Myers 1988; Schiøtte et al. 1989; Bowring et al. 1989; Song et al. 1996; Kinny and Nutman 1996, Nutman et al. 1996, 2000; Bowring and Williams 1999, Mojzsis and Harrison 2002). All these rocks are in high-grade terrains, where they have mostly been affected by strong ductile deformation and variable degrees of in situ migmatisation, so that as now preserved, they are complex and chemically modified products of superimposed tectono-thermal events. The variable state of preservation and hence of chemical integrity of these key old materials can make them difficult targets for geochemical and isotopic investigations. Thus it is always necessary to single out the rare, best-preserved materials for geochemical tasks, by integrating field geology with geochemical approaches (e.g., Nutman et al. 1999; Bennett et al. 2002; Polat et al. 2002; Frei and Polat 2007).

When using the geochemistry of these ancient rocks to extract information on the early Earth, U/Pb zircon dating is the most reliable approach to constrain their ages. Zircon dating in the Eoarchaean rocks of the Nuuk region (Fig. 1) in southern West Greenland is summarised in Fig. 2. From field geology and SHRIMP (Sensitive High mass Resolution Ion MicroProbe) U/Pb zircon dating, Nutman et al. (1993, 1996, 1997a, 2000, 2002a) concluded that granitoids of several ages back to c. 3,850 Ma are present in the Complex. This SHRIMP-based conclusion grew out of earlier bulk zircon ID-TIMS (isotope dilution thermal ionisation mass spectrometry) dating of cross-cutting orthogneiss components in the north of the complex near the Isua supracrustal belt, which showed that plutonic rocks with different ages are present (Baadsgaard et al. 1986). There is now a consensus that different-aged plutonic components up to c. 3,800 Ma *are* present in the orthogneisses of the Complex. For example, dating of abundant 3,810 and 3,790 Ma tonalites with quartz diorites immediately south of the Isua supracrustal belt (Nutman et al. 1993, 1996, 1999, 2000) has been replicated by Crowley (2003) and Kamber et al. (2003) and the dating of 3,650 Ma granites cutting 3,700 Ma tonalites north of the Isua supracrustal belt (Baadsgaard et al. 1986; Nutman et al. 1993, 1996, 2000) has been replicated by Crowley et al. (2002).

One age for orthogneisses that remains contentious is 3,850 Ma (Whitehouse and Kamber 2005; Nutman et al. 2004 and references therein). The contention concerns how to interpret the oldest zircons within these rocks. The view taken by Nutman and co-workers is that for most migmatites with tonalitic palaeosome, the petrographic and geochronological data from their oldest zircon population(s) are interpreted to give the time when the igneous protolith(s) in the palaeosome are formed (Nutman et al. 2000). Whitehouse and co-workers have interpreted near identical zircon data in a different fashion, and although they now also consider the possibility that these oldest zircons show the presence of pre-3,800 Ma crustal components in the Itsaq Gneiss Complex, they strongly suggest that these zircons might represent xenocrystic grains in younger (c. 3,660 Ma) magmatic rocks (Whitehouse et al. 1999; Whitehouse and Kamber 2005). In addition to interpretation of the zircon data, there is continuing divergence of opinion on the field relationships. In discussing previous work (Nutman et al. 1997a, 2000; Mojzsis and Harrison 2002), Whitehouse and Kamber (2005) summarise some of their concerns as: ‘‘In the case of the much discussed Akilia locality, the question is clearly that of how old the relative field relationships are (which some interpret as igneous cross-cutting), and it is, therefore, critically important to test whether these rocks underwent significant, pervasive partial melting that would have obliterated older structural relationships pertaining to the original, magmatic emplacement.’’

The contentious gneisses are within the more strongly reworked southern part of the Complex, where the presence of neosome produced by in situ melting followed by strong deformation clouds their interpretation (e.g., Nutman et al. 1996, 2000). To date, contention has focussed on Akilia and neighbouring islands (Fig. 1). Nutman et al. (1993, 1996, 1997a, 2000, 2002) presented increasingly more detailed data that they interpreted as showing that c. 3,850 Ma (‘‘pre-

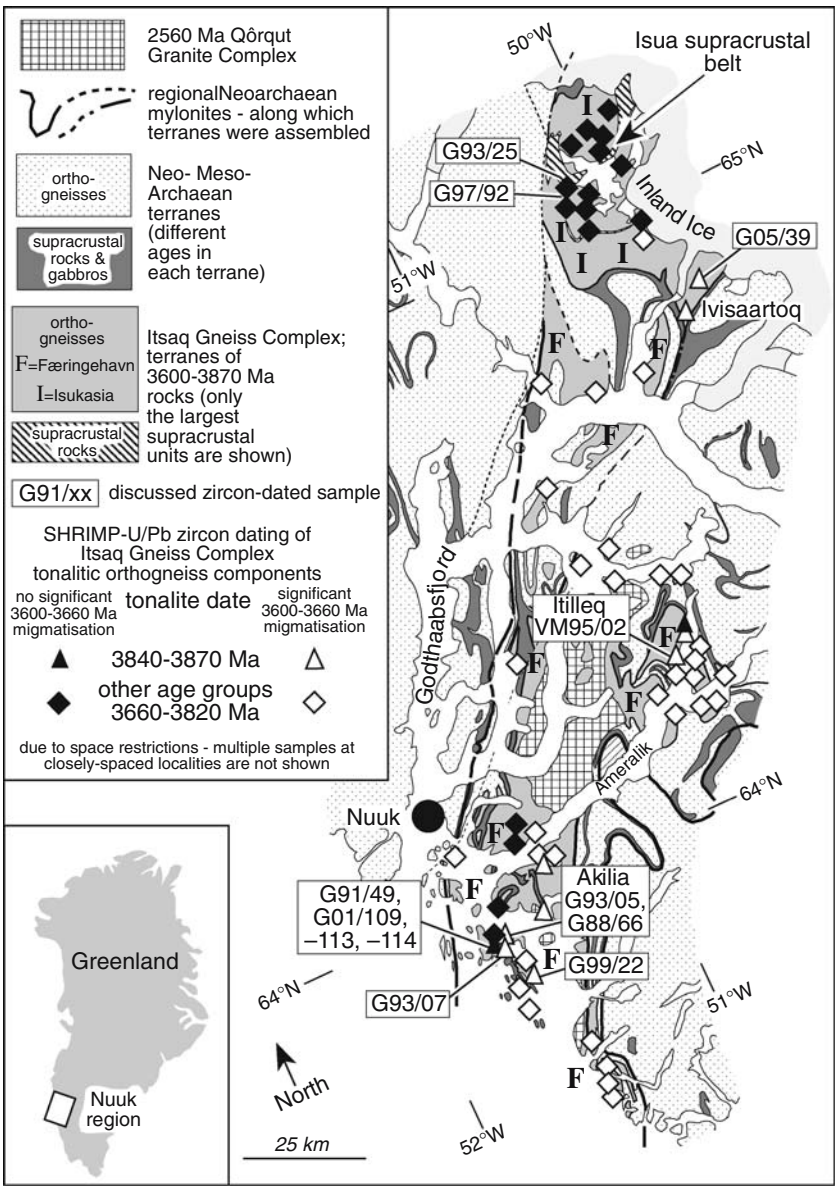

Fig. 1 Sketch geological map of the Itsaq Gneiss Complex in the Nuuk region, southern West Greenland, showing location of samples discussed

Isua'') rocks are present—variably and mostly strongly modified in superimposed tectonothermal events. These c. 3850 Ma zircon ages and the conclusion that they are crystallisation ages have been replicated by workers who used Cameca ion-microprobe zircon U/Pb dating, which included depth profiling (Mojzsis and Harrison 2002—working on a sample they recollected from the G93/05 sample locality from Nutman et al. 1997a) and by ID-TIMS zircon U/Pb dating (Krogh et al. 2002). These workers concluded that c. 3,850 Ma rocks are present. Whitehouse and Kamber (2005) also found c. 3,850 Ma zircons in an Akilia rock, and although not necessarily agreeing that they give the actual intrusion age of the rock, they did conclude that these zircons must demonstrate the presence of c. 3,850 Ma grey gneisses within the Itsaq Gneiss Complex.

The present paper first presents results from a small area of fortuitously well-preserved homogeneous metatonalite (Figs. 3 and 4), which we interpret to be 3,849±9 Ma old. Then, via a progression from almost homogeneous metatonalites to banded migmatitic gneisses, we demonstrate how c. 3,850 Ma rocks (Fig. 5) and their igneous zircons have been variably modified. This is a result of ductile deformation combined with in situ neosome production and veining during several post-3,850 Ma tectonothermal events, which makes it hard to recognise these oldest components (e.g. Nutman et al. 1996, 2000, 2002; Friend and Nutman 2005a). Via reconnaissance zircon dating of many migmatites, we show that c. 3,850 Ma zircons interpreted to date tonalitic palaeosome occur at several localities across the Complex (Fig. 1). Lastly, there are 3,850 Ma

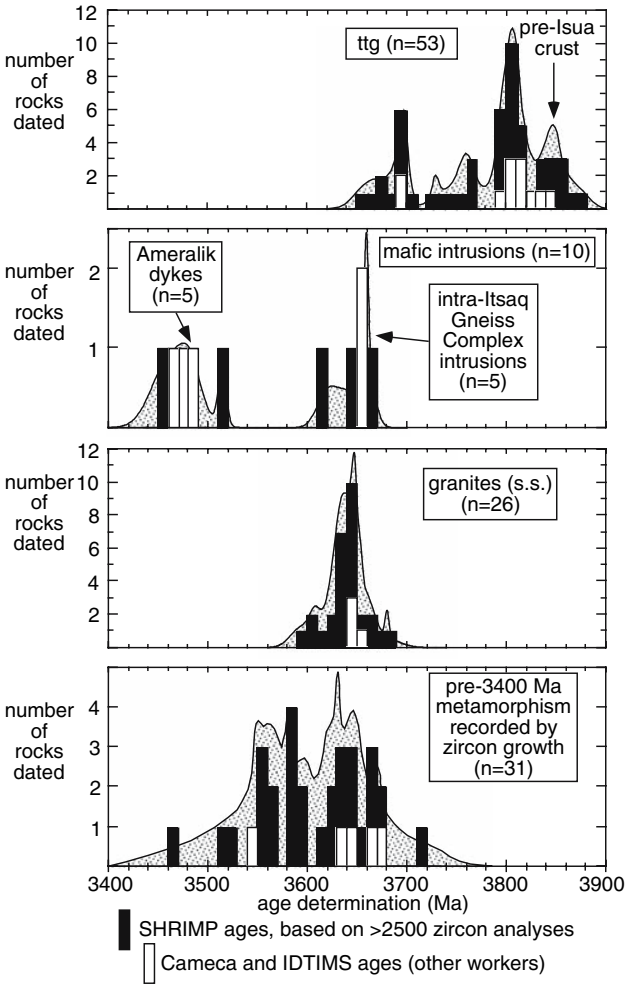

Fig. 2 Summary of zircon age determinations from the Itsaq Gneiss Complex. Each date on the histogram is based on multiple zircon analyses, with a total of at least 2,500 individual zircon analyses

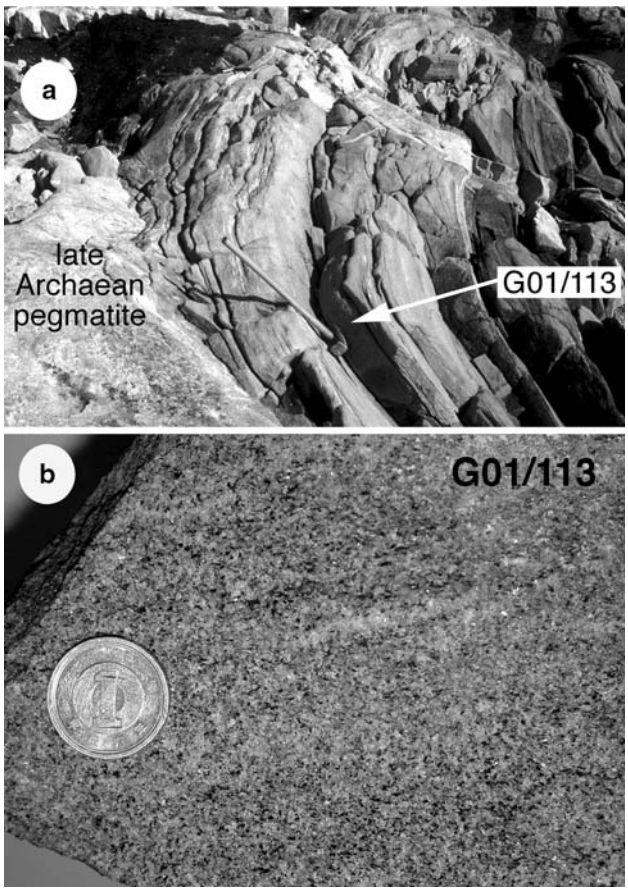

Fig. 3 **a** Field setting of meta-tonalite sample G01/113. **b** Sample G01/113, coin is 1 cm diameter

zircons derived from quartzo–feldspathic rocks found as xenocrysts within some 3,600–3,660 Ma granites sensu stricto (Friend and Nutman 2005a) and as detrital grains in c. 3,800 Ma detrital sediments (Nutman et al. 1997b). When combined, we interpret these data to demonstrate that a c. 3,850 Ma ''pre-Isua'' (i.e. pre-3,700–3,800 Ma) tonalitic crust is a widespread, albeit probably volumetrically minor component, within the Itsaq Gneiss Complex.

Eoarchaean Itsaq Gneiss Complex

Geological overview

The Eoarchaean rocks of the Nuuk region, Greenland (Black et al. 1971; Moorbath et al. 1972; Baadsgaard 1973) are mainly quartzo–feldspathic gneisses (formerly the *Amîtsoq gneisses*, McGregor 1973) that were derived from several generations of petrogenetically diverse diorites, tonalites, trondhjemites (TTG suite rocks) and granites (e.g. O'Nions and Pankhurst 1974; McGregor 1979; Baadsgaard et al. 1986; Nutman and Bridgwater 1986; Nutman et al. 1984, 1996, 1999, 2000; Crowley et al. 2002; Crowley 2003). The term *Itsaq Gneiss Complex* embraces all the Eoarchaean rocks of the Nuuk region (Nutman et al. 1996). The largest body of basic, ultramafic and metasedimentary rocks in the Complex is the c. 35 km long *Isua supracrustal belt* (e.g. Moorbath et al. 1973; Bridgwater and McGregor 1974; Allaart 1976 for the first studies and Nutman et al. 1997b; Maruyama et al. 1992; Komiya et al. 1999; Rosing 1999; Polat et al. 2002 for examples of new work). Smaller higher-grade bodies dominated by amphibolite occur throughout the rest of the Complex. These are similar to, although not necessarily contemporaneous with, mafic rocks of the Isua supracrustal belt (Nutman et al. 1996).

The Itsaq Gneiss Complex is cut by the Mesoarchaean Ameralik dykes (McGregor 1973; Gill and Bridgwater 1979; Chadwick 1981; Nielsen et al. 2002; Nutman et al. 2004a). It is tectonically intercalated with terranes of Neoarchaean gneisses devoid of Eoarchaean material and is also intruded by younger bodies of crustally derived granite (Friend et al. 1987, 1988, 1996; McGregor et al.

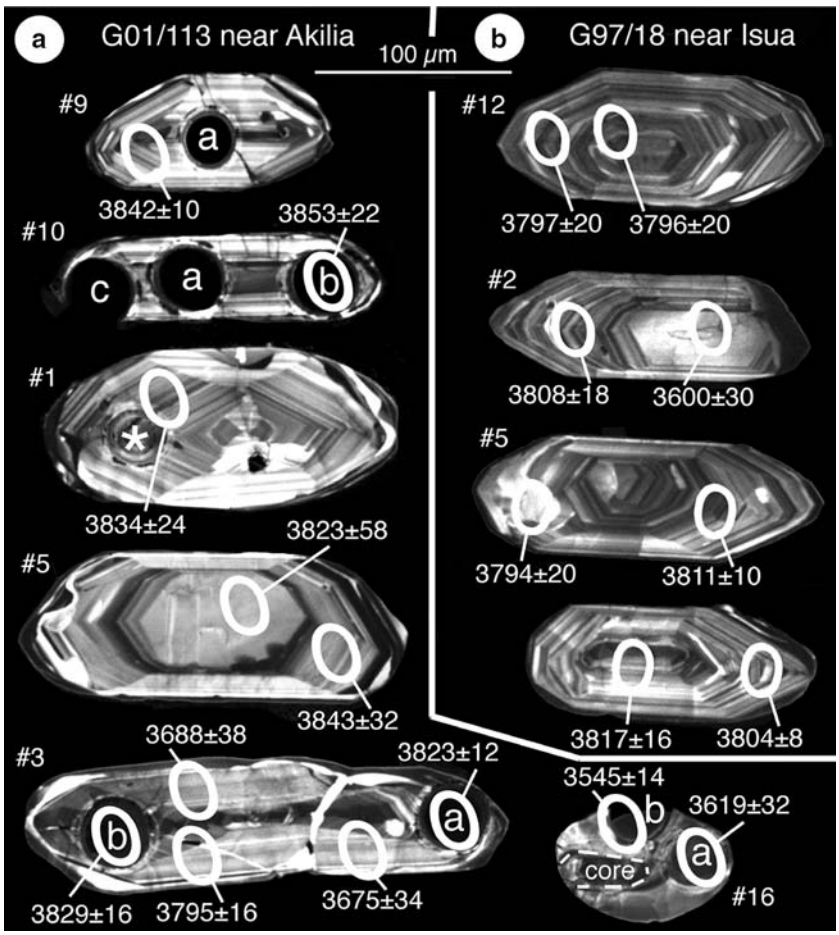

Fig. 4 **a** CL images of zircons from G01/113. Grain 16 is the only grain out of c. 140 mounted that has a rim broad enough (>10 μm) for SHRIMP analysis. The *dark spots* on the grains labelled *a*, *b*, *c* are pits created by LA-ICP-MS analysis. Site * is a mark on a grain made when checking the position of the laser beam, but no analysis was made. **b** CL images of zircons from c. 3810 Ma metatonalite sample G97/18 from near Isua (after Nutman et al. 1999). SHRIMP analysis sites are shown by *white ellipses* and $^{207}Pb/^{206}Pb$ dates are given with analytical errors at the 2σ level

1991; Crowley 2002; Friend and Nutman 2005b). The Complex is now considered to consist of separate tectonic slices—the *Færingehavn terrane* in the south (indicated by F's on Fig. 1), and the *Isukasia terrane* in the north (indicated by I's on Fig. 1), that are interpreted to have been brought into their present disposition during several later Archaean tectonic events (Friend and Nutman 2005b).

Heterogeneous strain and migmatisation

At most localities in the Itsaq Gneiss Complex, detailed field evidence for the Eoarchaean evolution of the rocks has been obliterated by strong polyphase ductile deformation during Neoarchaean terrane assembly events (McGregor 1973; Friend et al. 1987, 1988; McGregor et al. 1991; Nutman et al. 1996, 2000; Crowley 2002). During these events the originally cross-cutting Ameralik dykes were mostly transformed into sub-concordant, disrupted tabular amphibolites (McGregor 1973; Chadwick and Nutman 1979; McGregor et al. 1991). However, there are small low-strain domains in the Complex where the Ameralik dykes still cross-cut relatively undeformed Eoarchaean country rocks. The largest of these domains are in the northern end of the Complex near to the Isua supracrustal belt and show cross-cutting relationships preserved between the plutonic protoliths of the orthogneisses (e.g., Bridgwater and McGregor 1974; Nutman and Bridgwater 1986; Nutman et al. 1996, 1999; White et al. 2000; Crowley et al. 2002).

In contrast, in smaller domains of lower Neoarchaean strain in the southern part of the Complex, Ameralik dykes (dated at >3,450 Ma—Nutman et al. 2004) cut Eoarchaean migmatitic layering and in situ felsic segregations that were probably derived from arrested partial melting (e.g., Nutman et al. 1996, 2002; McGregor et al. 2000; Friend and Nutman 2005a). This Eoarchaean in situ incipient partial melting and migmatisation is correlated with textural and rare mineralogical observations such as pre-Ameralik dyke relict metamorphic orthopyroxene (metamorphic orthopyroxene in the Itsaq Gneiss Complex rocks variably replaced by amphibole + quartz ± biotite; criteria in McGregor and Friend 1997) interpreted to reflect Eoarchaean granulite facies metamorphism (McGregor and Mason 1977; Griffin et al. 1980; McGregor 2000; Friend and Nutman 2005a). This migmatisation and higher-grade metamorphism compound the difficulties in the interpretation of geochemical and isotopic data for the Eoarchaean rocks.

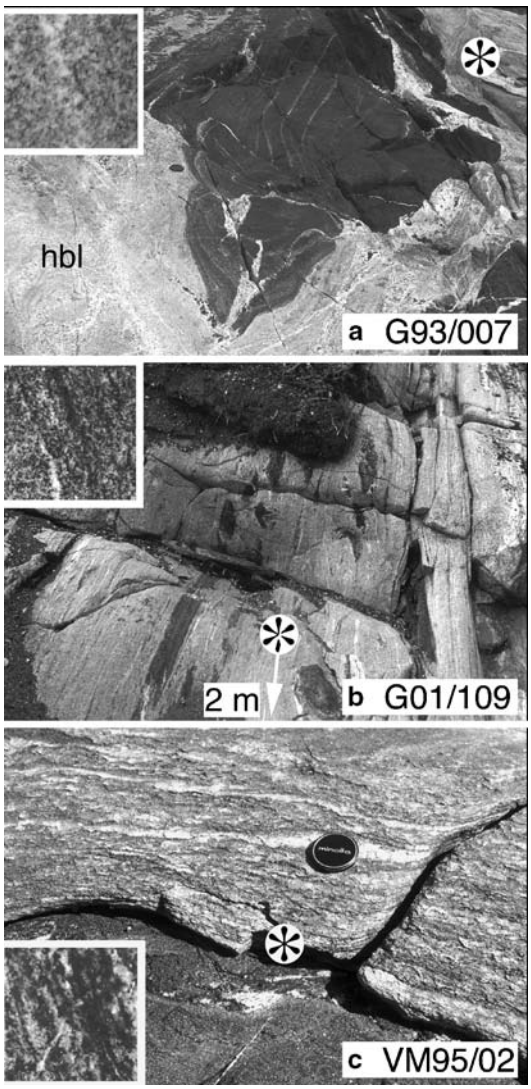

Fig. 5 Variable state of non-homogeneous rocks from the Itsaq Gneiss Complex with c. 3850 Ma zircons. **a** G93/07 weakly deformed metatonalite with some nebulitic felsic segregation patches. **b** G01/109 weakly banded gneiss with some pegmatites. **c** VM95/02 neosome-rich migmatite

A major goal of our studies on the southern part of the Itsaq Gneiss Complex has been to establish the age and identity of the protoliths that suffered variable amounts of in situ melting during granulite facies metamorphism. By building upon our complete mapping of Akilia and the adjacent islands and mainland coast on mapping at scales of 1:10,000 to 1:100 (Nutman 1980; Friend et al. 1987; Nutman et al. 2002), weakly deformed small domains in the southern migmatites that locally are even free of evidence of in situ partial melting have been identified (Nutman et al. 2000, 2002). In these domains, rare cross-cutting Eoarchaean plutonic relationships are still preserved, albeit distorted by superimposed ductile deformation (Nutman et al. 2000, 2002). Such domains are the source of very rare, best-preserved 3,850 Ma tonalites (sample G01/113; Figs. 3, 4). In this paper, the progression of samples from slightly heterogeneous/nebulous tonalite (G93/07) to veined tonalite (G01/109) to banded gneiss migmatites (VM95/02 and G05/39) illustrates how c. 3,850 Ma rocks have been modified and largely obscured as one of several age components within the banded gneisses of the Itsaq Gneiss Complex. Field photographs of three variably preserved rocks (G93/07, G01/109, VM95/02) are given in Fig. 5 to illustrate this transformation. The data repository (see Electronic Supplementry Material) contains petrographic descriptions, the SHRIMP U/Pb zircon data (Table R1) and the SHRIMP U/Pb zircon analytical method.

Well-preserved c. 3,850 Ma rocks

G01/113—best preserved, single age component c. 3,850 Ma rock

G01/113 is situated on the southeastern side of the same island c. 1 km west of Akilia as samples G91/49 (Nutman et al. 1996, 2000) and G01/114 (Nutman et al. 2002). Sample G01/113 is from a c. 30 cm thick horizon of massive tonalite, present just above high tide level (63°55.68′N, 51°43.60′W—WGS-84 datum) (Fig. 3a). The sample G01/113 is only weakly foliated and has very few small felsic veins (Fig. 3b). The most homogeneous character of this rock is maintained over only a few m^2 of outcrop. The protolith characteristics of this sample are better preserved than those previously discussed G91/49, G93/05, G99/22 and G01/114 (Nutman et al. 1997a, 2000, 2002).

G01/113 yielded *only* prismatic, lilac-coloured zircons, with *no* ovoid/multi-faceted grains, like those identified in the other relatively homogeneous metatonalites to which we ascribe a c. 3,850 Ma age (G91/49, G93/05, G99/22, G01/114, Nutman et al. 1997a, 2000, 2002). CL imaging indicates the G01/113 zircons have oscillatory zoning parallel to the grain exteriors (Fig. 4a). Many grains have an incomplete thin (≤ 5 μm) skin of structureless to weakly zoned zircon. However, of the 140 zircons mounted and CL-imaged, only one (grain 16, Fig. 4a) had a broad enough rim (>20 μm) for SHRIMP U/Pb spot dating. G01/113 with its single generation of oscillatory zoned (igneous) zircon (but partly modified by some recrystallisation) plus very restricted development of (metamorphic) rims possesses an unusually simple zircon population for a sample from the southern end of the Itsaq Gneiss Complex. The morphology of G01/113 zircons (Fig. 4a) closely resembles those of zircons from c. 3,810 Ma tonalites and quartz-diorites south of Isua (sample G97/18; Fig. 4b), which are widely interpreted to give the age for the rocks

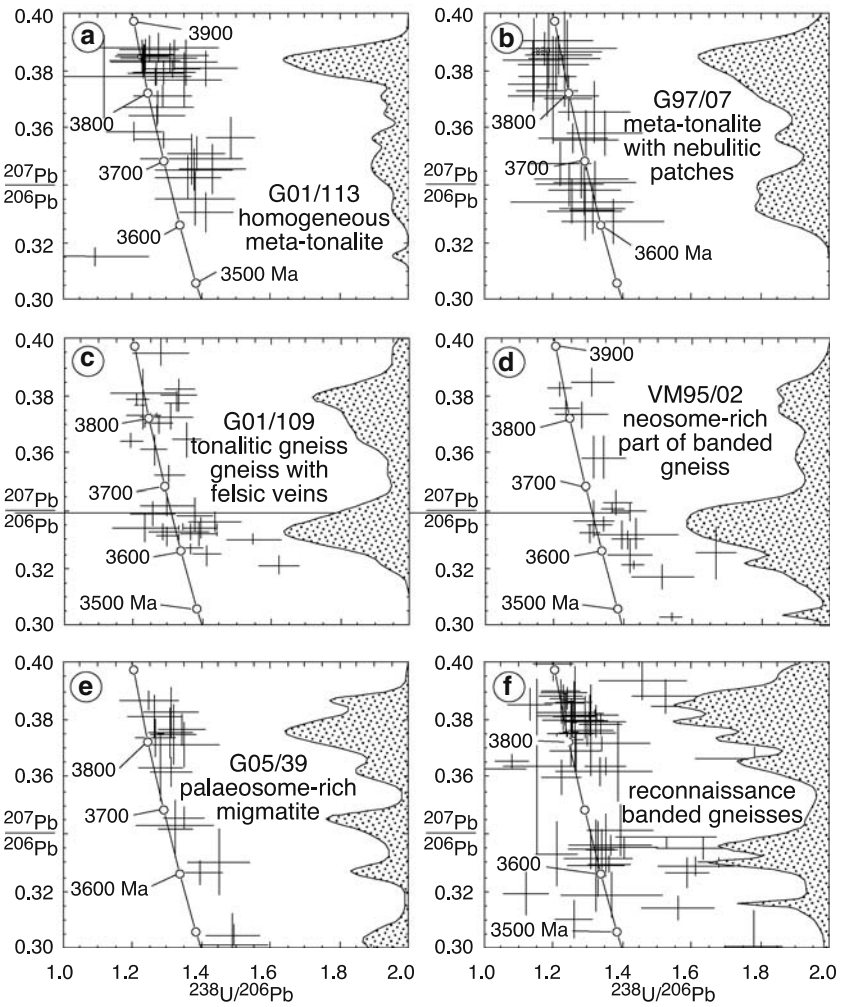

Fig. 6 $^{238}U/^{206}Pb$ vs. $^{207}Pb/^{206}Pb$ concordia diagrams with errors depicted at the 2σ level. On the right-hand side of each frame is shown the cumulative probability distribution for $^{207}Pb/^{206}Pb$ of the data set

rather than for an inherited component (Nutman et al. 1999; Crowley 2003; Kamber et al. 2003).

SHRIMP U/Pb zircon analyses for G01/113 zircons (Table 1) are summarised in a $^{238}U/^{206}Pb$–$^{207}Pb/^{206}Pb$ plot (Fig. 6a). Analyses of oscillatory-zoned zircon have Th/U ratios between 0.19 and 0.74, with most >0.4. Their ages are mostly concordant within error, with the majority of analyses giving $^{207}Pb/^{206}Pb$ dates of >3,800 Ma. Where $^{207}Pb/^{206}Pb$ dates of <3,800 Ma were obtained from the first analysis of a grain, multiple analysis on the same grain (e.g. grains 3, 6 and 11) found sites with ages >3,800 Ma. This demonstrates that the spread of $^{207}Pb/^{206}Pb$ dates in the oscillatory-zoned zircon is due to ancient loss of radiogenic Pb from >3,800 Ma grains. Applying an ancient radiogenic Pb loss interpretation to explain the dispersion in the $^{207}Pb/^{206}Pb$ dates, those with the ''oldest'' dates and statistically indistinguishable from each other, yielded a weighted mean $^{207}Pb/^{206}Pb$ date of 3,849±6 Ma (95% confidence; obtained by culling of ''young'' domains until MSWD < 1 for the remaining group—using the program ''Isoplot'' of Ludwig 1997). The only possible exception to this 3,849 Ma age is grain 15, where sites with $^{207}Pb/^{206}Pb$ dates up to c. 3,750 Ma were found. This could be a >3,800 Ma grain with greater ancient loss of radiogenic Pb, or it could be a rare c. 3,750 Ma grain, perhaps from the few thin felsic veins in the otherwise homogeneous sample (Fig. 3b). Two analyses of the only rim broad enough to take a c. 20 μm SHRIMP spot (Fig. 4a) is devoid of oscillatory zoning in CL imaging and gave young $^{207}Pb/^{206}Pb$ dates of 3,619±16 and 3,545±7 Ma (1σ), with lower Th/U of c. 0.2.

The chemistry of G01/113 zircons was also examined by Laser Ablation Inductively Coupled Plasma Mass Spectrometry Table 2, (LA-ICP-MS—analytical method and data processing are summarised in data repository (see Electronic Supplementry Material), where the data are also lodged as Table R2). Where LA-ICP-MS analyses were initiated over (c. 1 μm deep), SHRIMP dating sites, there was good correspondence between the SHRIMP $^{207}Pb/^{206}Pb$ ratio and the LA-ICP-MS $^{207}Pb/^{206}Pb$ ratio at the start of the profile. The prior extensive SHRIMP U/Pb dating of these zircons indicates that they have negligible

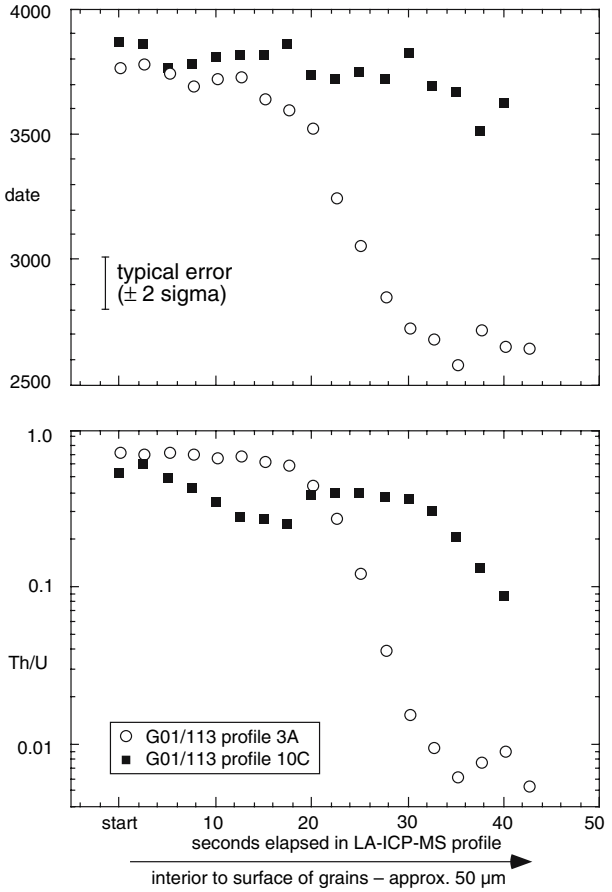

Fig. 7 Laser ablation ICP-MS analysis profiles 3A and 10C through the edges of two zircons in metatonalite G01/113 **a** $^{207}Pb/^{206}Pb$ date age and **b** Th/U ratio. Typical error on the $^{207}Pb/^{206}Pb$ date for each 2.5 s segment is ±50 Ma (2σ—C. Allen, personal communication, 2006)

amounts of ^{204}Pb. Therefore the LA-ICP-MS $^{207}Pb/^{206}Pb$ ratios can be taken as a proxy for the $^{207}Pb/^{206}Pb$ age of the domain. In G01/113 zircons, several depth profiles were undertaken to examine the very thin partial skins mantling oscillatory-zoned zircon that are observed in the CL images. In post-analysis CL images, the LA-ICP-MS sites show as black pits (Fig. 4a). In these depth profiles the analysis started in the interior of the zircon sectioned in half in the polished grain mount, and with time burrows down towards the grain exterior embedded in the epoxy. Analyses 3A and 10C were processed by breaking them into 2.5 s slices (Fig. 7; Table 2). In analysis 3A, a thin outer shell (30 to 40 s portion of the analysis) with a Neoarchaean $^{207}Pb/^{206}Pb$ age has a Th/U ratio almost two orders of magnitude less than that found in its Eoarchaean oscillatory-zoned substrate. The $^{207}Pb/^{206}Pb$ date at the start of this profile is between 3,800 and 3,700 Ma but multiple SHRIMP dates on this grain found >3,800 Ma domains and indicate that variable ancient Pb loss from a >3,800 Ma crystal has occurred (Fig. 4a; Tables 1, 2). In analysis 10A, change at the margin of the grain is neither so dramatic nor as clear, but there is a more than halving of Th/U, coupled with a reduction in apparent age. In grain 9 (Table 2) a thin (<5 µm) very low Th/U rim was detected at the end of the analysis, with a $^{207}Pb/^{206}Pb$ date of 2,577 Ma. The LA-ICP-MS profiling plus dating of the only rim in sample G01/113 broad enough to be accessible by SHRIMP spot analysis (c. 25 µm wide on grain 16) demonstrates that partial mantles of several previously recognised regional ages (c. 3,650 and Neoarchaean) are present on these 3,850 Ma oscillatory-zoned zircons. However, these are largely <5µm wide, are volumetrically very minor and have features such as low Th/U.

Bulk rock zircon-undersaturation and interpretation of 3,850 Ma zircons

Using the experimental data of Watson and Harrison (1983), Mojzsis and Harrison (2002) demonstrated that the magmatic precursor of their tonalite sample GR9716 from Akilia (their recollection of sample G93/05; Nutman et al. 1997a, 2000, 2002) would have been strongly undersaturated in zircon and thus unlikely to preserve any inheritance. The same argument also applies for 3,850 Ma homogeneous single-component metatonalites (Table 3), and also for those from Isua with ages of c. 3,800 Ma (Nutman et al. 1999) and c. 3,700 Ma (Nutman and Bridgwater 1986; data repository in Fig. R1 of Electronic Supplementry Material). The simplest, most consistent explanation is an igneous origin for the well-preserved prismatic oscillatory-zoned zircons in these homogeneous metatonalites of different age. In contrast, in complex migmatites such as G91/33, interpreted as banded gneisses containing copious c. 3,650 Ma partial melt (Nutman et al. 1996, 2000), corroded, pre-3,650 Ma zircon of several ages back to c. 3,850 Ma is encountered. This is interpreted to indicate that when c. 3,650 Ma partial melts were produced in situ in these rocks, there was partial dissolution of the older zircons. This is in accord with the study of Watson (1996), who demonstrated that partial melt segregations should commonly carry some protolith zircon as inherited, partly resorbed cores mantled by new igneous zircon.

Whole rock major and trace element data for well-preserved 3,850 Ma rocks

In Fig. 8, the geochemistry of the five ''best'' 3,850 Ma rocks (plotted as solid diamonds) are compared to the average composition for >3,500 Ma TTG, and the trends depicted by the complete data set given by Martin et al. (2005). Also shown (as open triangles) are the 3,810 and 3,795 Ma rocks from Nutman et al. (1999). The c.

Table 1 SHRIMP U/Pb zircon analyses

Labels	Grain type	U (ppm)	Th (ppm)	Th/U	Comm. 206Pb%	$^{238}U/^{206}Pb$ ratio	$^{207}Pb/^{206}Pb$ ratio	207/206 date (Ma)	% disc
G01/113 meta-tonalite									
1.1	e,osc,p	181	75	0.42	0.075	1.412 ± 0.046	0.3807 ± 0.0031	3834 ± 12	–10
2.1	e,osc,p	215	147	0.69	0.067	1.322 ± 0.049	0.3853 ± 0.0026	3853 ± 10	–6
3.1	m,osc,p	135	51	0.38	0.124	1.287 ± 0.042	0.3709 ± 0.0019	3795 ± 8	–2
3.2	m,osc,p	165	74	0.45	0.103	1.361 ± 0.047	0.3427 ± 0.0037	3675 ± 17	–3
3.3	m,osc,p	133	41	0.30	0.038	1.432 ± 0.048	0.3456 ± 0.0043	3688 ± 19	–7
3.4	e,osc,p	340	236	0.69	0.020	1.291 ± 0.045	0.3794 ± 0.0021	3829 ± 8	–3
3.5	e,osc,p	312	150	0.48	0.056	1.267 ± 0.051	0.3778 ± 0.0014	3823 ± 6	–2
4.1	m,osc,p	160	77	0.48	0.005	1.248 ± 0.043	0.3874 ± 0.0023	3861 ± 9	–2
5.1	m,osc,p	121	49	0.41	0.611	1.117 ± 0.059	0.3779 ± 0.0073	3823 ± 29	8
5.2	e,osc,p	131	47	0.36	0.035	1.356 ± 0.046	0.3828 ± 0.0039	3843 ± 16	–7
6.1	m,osc,bip	176	91	0.52	0.039	1.273 ± 0.051	0.3672 ± 0.0028	3780 ± 11	–1
6.2	e,osc/rex,bip	164	73	0.44	0.023	1.381 ± 0.058	0.3353 ± 0.0047	3642 ± 22	–4
6.3	e,osc,bip	201	134	0.67	0.029	1.236 ± 0.051	0.3835 ± 0.0017	3846 ± 7	–1
7.1	e,osc,p	169	75	0.44	0.056	1.269 ± 0.041	0.3789 ± 0.0020	3827 ± 8	–2
8.1	e,osc,p	152	62	0.41	0.004	1.350 ± 0.054	0.3768 ± 0.0047	3819 ± 19	–6
9.1	e,osc,p	190	103	0.54	0.026	1.229 ± 0.047	0.3827 ± 0.0026	3842 ± 10	0
10.1	e,osc,p	208	91	0.44	0.001	1.238 ± 0.041	0.3854 ± 0.0027	3853 ± 11	–1
11.1	e,osc/rex,p,fr	207	87	0.42	0.001	1.272 ± 0.041	0.3642 ± 0.0018	3768 ± 7	–1
11.2	m,osc,p,fr	178	86	0.48	0.082	1.235 ± 0.034	0.3834 ± 0.0028	3845 ± 11	–1
11.3	e,osc/rex,p,fr	197	86	0.44	0.019	1.289 ± 0.042	0.3558 ± 0.0014	3732 ± 6	–1
11.4	e,osc,p,fr	222	102	0.46	0.027	1.232 ± 0.033	0.3842 ± 0.0024	3848 ± 10	0
12.1	e,osc,p	180	95	0.53	0.034	1.317 ± 0.039	0.3805 ± 0.0015	3834 ± 6	–5
13.1	e,osc,p	158	74	0.47	0.039	1.385 ± 0.042	0.3509 ± 0.0030	3711 ± 13	–6
13.2	m,osc,p	168	89	0.53	0.005	1.276 ± 0.086	0.3880 ± 0.0025	3863 ± 10	–3
13.3	e,osc,p	187	95	0.51	0.048	1.227 ± 0.038	0.3848 ± 0.0029	3851 ± 11	0
14.1	e,osc,p/bip	177	99	0.56	0.059	1.310 ± 0.038	0.3842 ± 0.0026	3848 ± 10	–5
15.1	m,osc,p/bip	144	62	0.43	0.001	1.484 ± 0.035	0.3564 ± 0.0036	3735 ± 15	–11
15.2	m,osc,p/bip	272	202	0.74	0.067	1.204 ± 0.040	0.3585 ± 0.0016	3744 ± 7	4
15.3	e,osc,p/bip	406	272	0.67	0.007	1.378 ± 0.056	0.3454 ± 0.0036	3687 ± 16	–5
15.4	e,osc,p/bip	286	167	0.59	0.058	1.371 ± 0.074	0.3490 ± 0.0044	3703 ± 19	–5
16.1	r,h,ov	186	36	0.19	0.096	1.413 ± 0.039	0.3305 ± 0.0034	3619 ± 16	–5
16.2	r,h,ov	202	40	0.20	0.209	1.092 ± 0.078	0.3150 ± 0.0015	3545 ± 7	18
G93/07 meta-tonalite with nebulitic patches									
1.1	e,osc,p[a]	38	15	0.40	0.181	1.232 ± 0.076	0.3875 ± 0.0032	3861 ± 13	–1
2.1	e,osc,p[a]	46	32	0.69	0.119	1.183 ± 0.044	0.3727 ± 0.0045	3803 ± 18	4
3.1	m,osc,p[a]	27	18	0.66	0.144	1.320 ± 0.059	0.3408 ± 0.0036	3666 ± 16	–1
3.2	e,osc,p[a]	32	12	0.37	0.292	1.144 ± 0.044	0.3833 ± 0.0072	3845 ± 29	5
4.1	e,osc,p[a]	36	19	0.51	0.158	1.294 ± 0.047	0.3556 ± 0.0052	3731 ± 22	–1
5.1	e,osc,p[a]	40	6	0.15	0.090	1.319 ± 0.052	0.3653 ± 0.0053	3772 ± 22	–4
6.1	e,osc,p	52	1	0.02	0.001	1.374 ± 0.074	0.3271 ± 0.0038	3604 ± 18	–2
7.1	m,osc,p[a]	40	19	0.49	0.085	1.200 ± 0.065	0.3709 ± 0.0083	3795 ± 34	3
8.1	e,osc,p[a]	38	15	0.39	0.037	1.216 ± 0.048	0.3852 ± 0.0034	3852 ± 14	0
9.1	e,osc,p[a]	33	16	0.49	0.201	1.174 ± 0.056	0.3875 ± 0.0028	3861 ± 11	3
10.1	e,osc,p[a]	99	58	0.59	0.084	1.258 ± 0.049	0.3563 ± 0.0025	3734 ± 11	1
10.2	m,osc,p[a]	36	26	0.71	0.362	1.183 ± 0.041	0.3779 ± 0.0039	3823 ± 16	3

Table 1 continued

Labels	Grain type	U (ppm)	Th (ppm)	Th/U	Comm. 206Pb%	$^{238}U/^{206}Pb$ ratio	$^{207}Pb/^{206}Pb$ ratio	207/206 date (Ma)	% disc
11.1	c,osc,p	27	17	0.63	0.139	1.233 ± 0.052	0.3840 ± 0.0082	3847 ± 33	0
11.2	r,h/sz,p	44	18	0.41	0.120	1.292 ± 0.053	0.3309 ± 0.0051	3621 ± 24	2
11.3	r,h/sz,p	33	12	0.37	0.365	1.291 ± 0.052	0.3383 ± 0.0043	3655 ± 20	1
12.1	outer r,h/sz	51	25	0.49	0.374	1.313 ± 0.047	0.3316 ± 0.0043	3624 ± 20	1
12.2	inner r,h/sz	35	15	0.43	0.083	1.282 ± 0.068	0.3419 ± 0.0032	3671 ± 14	1
12.3	c,osc,p	88	77	0.88	0.058	1.140 ± 0.036	0.3750 ± 0.0046	3812 ± 18	7
13.1	e,osc,p	40	33	0.83	0.148	1.142 ± 0.040	0.3833 ± 0.0035	3845 ± 14	6
14.1	e,osc,p	49	26	0.53	0.048	1.239 ± 0.050	0.3864 ± 0.0054	3857 ± 21	–1
15.1	r,hd/sz,p	208	10	0.05	0.097	1.254 ± 0.089	0.3342 ± 0.0037	3636 ± 17	4
16.1	e,osc,p	38	24	0.63	0.018	1.200 ± 0.051	0.3820 ± 0.0049	3840 ± 19	2
17.1	e,osc,p	40	21	0.54	0.323	1.209 ± 0.038	0.3821 ± 0.0046	3840 ± 18	1
18.1	e/r,sz,p	150	4	0.02	0.016	1.314 ± 0.032	0.3312 ± 0.0029	3622 ± 13	1
19.1	e,osc,p	26	12	0.46	0.181	1.188 ± 0.063	0.3902 ± 0.0082	3872 ± 32	2
20.1	e,osc/rex,p	44	8	0.18	0.201	1.220 ± 0.044	0.3472 ± 0.0039	3695 ± 17	4
21.1	e,osc,p	65	2	0.03	0.063	1.248 ± 0.049	0.3401 ± 0.0038	3663 ± 17	4
22.1	e,osc,p	63	31	0.49	0.096	1.244 ± 0.034	0.3703 ± 0.0039	3792 ± 16	0
23.1	e,osc,p	37	16	0.43	0.049	1.349 ± 0.054	0.3580 ± 0.0038	3742 ± 16	–4
G01/109 tonalitic gneiss with segregations and veins									
1.1	m,osc,p	100	36	0.36	0.149	1.621 ± 0.059	0.3210 ± 0.0031	3575 ± 15	–13
2.1	e,osc,p,fr	292	216	0.74	0.082	1.328 ± 0.053	0.3804 ± 0.0054	3833 ± 22	–6
3.1	e,osc,p	74	40	0.54	0.074	1.332 ± 0.046	0.3822 ± 0.0030	3840 ± 12	–6
4.1	e,osc,p	139	58	0.42	0.043	1.323 ± 0.036	0.3775 ± 0.0027	3822 ± 11	–5
5.1	e,osc,p	231	40	0.17	0.104	1.296 ± 0.079	0.3415 ± 0.0035	3670 ± 16	1
5.2	m,osc,p	100	36	0.36	0.079	1.352 ± 0.042	0.3646 ± 0.0061	3769 ± 26	–5
5.3	m,osc,p	198	38	0.19	0.027	1.549 ± 0.079	0.3301 ± 0.0020	3617 ± 10	–11
5.4	m,osc,p	142	77	0.54	0.021	1.221 ± 0.043	0.3732 ± 0.0048	3805 ± 20	1
6.1	e,osc,p	87	35	0.40	0.292	1.411 ± 0.041	0.3245 ± 0.0035	3591 ± 17	–4
7.1	e,osc,p,fr	107	33	0.31	0.099	1.258 ± 0.038	0.3611 ± 0.0054	3754 ± 23	0
8.1	m,osc,p	111	59	0.53	0.116	1.276 ± 0.084	0.3952 ± 0.0046	3891 ± 18	–4
8.2	c,osc,p	93	41	0.44	0.099	1.226 ± 0.097	0.3807 ± 0.0084	3834 ± 34	0
8.3	r,h,p	102	46	0.45	0.112	1.435 ± 0.074	0.3362 ± 0.0033	3645 ± 15	–6
8.4	c,osc,p	115	58	0.50	0.048	1.226 ± 0.036	0.3807 ± 0.0038	3835 ± 15	0
8.5	r,osc,p	96	45	0.47	0.089	1.255 ± 0.065	0.3390 ± 0.0041	3658 ± 18	3
9.1	e,osc,p	146	64	0.44	0.001	1.208 ± 0.034	0.3792 ± 0.0021	3828 ± 8	2
10.1	e,osc,p	117	31	0.26	0.102	1.302 ± 0.043	0.3520 ± 0.0035	3716 ± 15	–1
11.1	e,osc,p	81	48	0.59	0.193	1.307 ± 0.061	0.3729 ± 0.0044	3803 ± 18	–4
12.1	m,hd,bip	148	72	0.48	0.245	1.392 ± 0.048	0.3342 ± 0.0036	3637 ± 17	–4
13.1	e,osc,p/bip	178	35	0.20	0.102	1.190 ± 0.032	0.3644 ± 0.0027	3768 ± 11	4
14.1	e,osc,p	120	63	0.52	0.045	1.272 ± 0.040	0.3703 ± 0.0030	3793 ± 13	–1
15.2	e,osc,p	174	91	0.53	0.457	1.297 ± 0.035	0.3309 ± 0.0030	3621 ± 14	2
16.1	e,hd,ov	81	32	0.39	0.281	1.388 ± 0.054	0.3320 ± 0.0044	3626 ± 20	–4
16.2	e,hd,ov	85	36	0.42	0.109	1.367 ± 0.051	0.3324 ± 0.0029	3628 ± 14	–2
17.1	e,hd,ov	72	31	0.43	0.121	1.281 ± 0.042	0.3326 ± 0.0029	3629 ± 13	3
17.2	e,hd,ov	72	39	0.53	0.120	1.379 ± 0.053	0.3383 ± 0.0060	3655 ± 28	–4
18.1	m,hd,ov	141	67	0.48	0.063	1.362 ± 0.039	0.3269 ± 0.0017	3602 ± 8	–1
18.2	e,hd,ov	341	176	0.52	0.426	1.232 ± 0.095	0.3339 ± 0.0049	3635 ± 22	5

Table 1 continued

Labels	Grain type	U (ppm)	Th (ppm)	Th/U	Comm. 206Pb%	$^{238}U/^{206}Pb$ ratio	$^{207}Pb/^{206}Pb$ ratio	207/206 date (Ma)	% disc
VM95/02 schlieric migmatite with abundant neosome									
1.1	m,osc,p,f	62	67	1.075	0.455	1.778 ± 0.040	0.2316 ± 0.0020	3063 ± 14	–6
2.1	e,osc/h,p	120	36	0.302	0.086	1.342 ± 0.027	0.3355 ± 0.0025	3642 ± 11	–1
2.2	m,osc,p	111	88	0.794	0.001	1.315 ± 0.105	0.3394 ± 0.0041	3660 ± 18	0
3.1	m,h/rex,eq	63	27	0.425	0.190	1.369 ± 0.031	0.3407 ± 0.0023	3666 ± 10	–3
3.2	m,h/rex,eq	51	21	0.405	0.017	1.514 ± 0.090	0.3170 ± 0.0044	3555 ± 21	–8
4.1	m,osc,p	99	44	0.450	0.048	1.218 ± 0.034	0.3825 ± 0.0024	3842 ± 10	1
4.2	m/e,osc,p	268	61	0.227	0.020	1.232 ± 0.043	0.3758 ± 0.0030	3815 ± 12	0
4.3	m,osc,p	67	31	0.472	0.089	1.311 ± 0.060	0.3850 ± 0.0048	3851 ± 19	–5
5.1	m,rex/hd,p	285	30	0.105	0.006	1.428 ± 0.031	0.3213 ± 0.0014	3576 ± 7	–4
6.1	m,osc/rex,p	42	25	0.582	0.049	1.379 ± 0.036	0.3430 ± 0.0042	3676 ± 19	–4
6.2	m,osc,p	83	34	0.410	0.002	1.315 ± 0.056	0.3364 ± 0.0040	3647 ± 18	0
7.1	e,osc,p	83	29	0.351	0.039	1.302 ± 0.028	0.3321 ± 0.0033	3627 ± 15	1
8.1	m,osc,p	124	56	0.450	0.006	1.313 ± 0.032	0.3586 ± 0.0074	3744 ± 32	–2
8.2	m,osc,p	184	68	0.367	0.044	1.280 ± 0.075	0.3733 ± 0.0044	3805 ± 18	–2
8.3	e,osc,p	30	38	1.262	0.983	1.457 ± 0.130	0.2877 ± 0.0075	3405 ± 41	–1
9.1	m,osc/h,p,f	317	56	0.176	0.034	1.539 ± 0.031	0.3031 ± 0.0011	3486 ± 6	–7
10.1	m/e,osc,p	71	37	0.525	0.067	1.413 ± 0.046	0.3300 ± 0.0030	3617 ± 14	–5
11.1	m,osc,p,f	70	39	0.552	0.036	1.394 ± 0.078	0.3318 ± 0.0049	3626 ± 23	–4
12.1	e,osc,p	65	31	0.479	0.084	1.439 ± 0.120	0.3320 ± 0.0054	3626 ± 25	–6
13.1	e,osc,p,f	32	47	1.457	1.111	1.669 ± 0.060	0.3252 ± 0.0090	3594 ± 43	–16
14.1	e,osc/hd,p	83	30	0.357	0.014	1.419 ± 0.062	0.3245 ± 0.0059	3591 ± 28	–4
15.1	e,osc,p	39	71	1.817	0.226	1.342 ± 0.065	0.3585 ± 0.0073	3743 ± 31	–4
16.1	m,p	75	50	0.664	0.001	1.417 ± 0.051	0.3398 ± 0.0033	3662 ± 15	–6
17.1	m,osc/rex,p	41	46	1.126	0.509	1.689 ± 0.174	0.2871 ± 0.0075	3402 ± 41	–12

See Nutman et al. (1996, 1997a, b, 1999, 2000, 2002) and Friend and Nutman (2005a) for data for samples; G88/66, G91/49, G93/05, G93/25, G97/18, G97/92, G99/22, G01/114 discussed in this paper; corrected with 3850 Ma model Pb of Cumming and Richards (1975)

p prismatic, *eq* equant and ovoid, *e* end, *m* middle, *r* overgrowth, *c* core, *rex* recrystallised, *osc* oscillatory finescale zoning, *s* sector zoning, *h* homogeneous, *hd* homogeneous dark, *f* fragment, *anh* anhedral, *turb* turbid

[a] Very thin (partial) mantle

3,850 Ma rocks correspond to typical Archaean high-Al TTG (Barker and Arth 1976) with SiO_2 > 68 wt%, alumina >15 wt% and with high Na_2O relative to K_2O, giving them a metaluminous character (Table 3; Fig. 8a—data repository, (see Electronic Supplementry Material) for analytical methods and data lodged as Table R3). They have low ferromagnesian components with low Cr and Ni. However, they also have low Sr (<350 ppm) and Ba (<125 ppm) and match the broad TTG definitions of Martin (1994) and Martin et al. (2005).

The c. 3,850 Ma rocks are characterised by relatively low overall REE abundances but which display steep, enriched LREE relative to HREE primitive mantle-normalised patterns with $(La/Yb)_N$ of >10) Table 3, (Fig. 8b, data repository Table R3), features which are consistent with garnet ± amphibole in the residues (e.g. Martin et al. 2005). Such patterns have been modelled for the c. 3,810 and c. 3,795 Ma TTG (Nutman et al. 1999) by up to 40% partial melting of a garnetiferous mafic source. Eu anomalies are small (Eu/Eu* = 0.8–1.6) (Table 3).

In terms of tectonic discrimination diagrams, the c. 3,850 Ma tonalites fall within the field of volcanic arc granites (VAG—Fig. 8c). As these rocks have been affected by c. 3,650 Ma granulite facies, potential Rb loss must be considered. However, the Rb concentrations of these rocks overlap those of the 3,810 and 3,795 Ma TTG that were only ever metamorphosed to amphibolite facies conditions (Nutman et al. 1999). This suggests that any modification has not grossly altered their Rb abundances. In terms of the secular trends versus SiO_2 (e.g. MgO, Na_2O + CaO, Cr, Ni and Sr), identified by Martin and Moyen (2002), Smithies et al. (1993) and Martin et al.

Table 2 LA-ICP-MS zircon trace element analyses

Analysis	Site	Date[a]	Th	U	P	Ca	Sr	Y	La	Ce	Pr	Nd	Sm	Eu	Gd	Tb	Dy	Ho	Er	Tm	Yb	Lu
G01/113 tonalite "depth profiling" (2.5 s segments)																						
Profile 3A																						
3A-start	0.0s (ig)	3767	276	380	132	bdl	0.89	826	7.32	53.17	4.50	36.02	20.54	3.75	54.81	12.1	96.32	28.55	111.70	22.85	201.16	35.50
	2.5s	3783	263	367	275	bdl	bdl	866	6.00	46.47	5.18	34.22	20.99	2.90	48.70	10.4	93.00	28.41	108.06	21.53	187.32	34.62
	5.0s	3746	225	303	451	bdl	bdl	686	4.97	43.41	3.43	20.64	14.71	2.62	36.98	8.0	81.92	25.33	99.85	19.83	169.77	30.23
	7.5s	3698	272	383	356	bdl	1.50	875	4.13	42.32	3.63	25.13	18.00	2.38	40.21	9.1	90.01	29.28	115.20	23.91	207.04	37.27
	10.0s	3724	259	385	495	bdl	bdl	958	7.21	57.56	5.62	35.56	23.02	3.43	50.65	11.9	100.88	32.16	127.73	25.31	210.28	39.80
	12.5s	3737	251	361	357	bdl	bdl	822	10.19	71.68	8.14	43.66	25.92	2.10	57.38	11.1	102.22	29.14	126.07	24.13	210.98	40.34
	15.0s	3645	220	341	526	bdl	1.42	766	6.59	43.72	4.26	23.10	12.86	2.13	42.62	8.6	85.53	23.71	112.77	21.20	188.24	37.89
	17.5s	3598	198	328	bdl	bdl	bdl	730	1.58	24.62	1.13	8.59	9.33	1.12	34.22	6.2	64.66	22.62	99.88	21.08	185.92	40.43
	20.0s	3531	163	363	116	bdl	bdl	699	2.06	28.24	1.92	16.22	8.70	1.46	25.67	7.2	64.91	22.21	99.81	21.42	226.56	46.63
	22.5s	3253	94	341	285	bdl	bdl	665	3.45	21.12	1.68	10.77	9.08	1.40	22.20	4.8	58.69	18.96	91.07	23.34	237.74	48.42
	25.0s	3059	44	357	135	bdl	bdl	608	1.75	14.34	0.73	8.61	5.42	0.77	17.56	4.0	42.92	17.26	94.02	24.21	265.13	55.71
	27.5s	2858	15	361	bdl	bdl	1.38	500	1.53	9.94	1.21	6.08	4.48	0.49	16.58	3.0	33.04	14.38	85.17	23.49	271.35	55.54
	30.0s	2734	6	382	bdl	bdl	bdl	419	0.79	8.57	1.11	5.54	2.98	0.70	10.49	1.2	27.22	11.52	70.24	20.78	251.62	53.89
	32.5s	2689	4	389	bdl	bdl	bdl	379	1.28	7.54	0.84	4.17	2.24	0.71	8.95	1.9	22.86	10.35	67.96	18.72	240.11	54.27
	35.0s	2587	3	404	bdl	0.89	bdl	400	3.00	6.96	0.51	2.75	3.16	0.45	5.77	1.5	20.39	10.77	62.61	19.59	217.15	53.78
	37.5s	2725	3	410	348	bdl	bdl	356	1.94	6.05	0.30	7.32	4.99	0.82	8.50	1.5	22.57	10.42	63.26	19.31	240.48	56.96
	40.0s	2662	4	446	bdl	bdl	bdl	413	1.95	10.01	1.25	3.90	4.00	1.08	6.86	1.7	29.14	11.21	73.47	19.95	261.93	59.55
3A-finish	42.5s (met)	2653	2	353	bdl	bdl	bdl	408	1.10	11.78	0.69	4.74	9.77	0.73	4.14	1.4	20.42	8.37	51.18	18.41	211.75	50.52
Profile 10C																						
10C start	0.0s (ig)	3863	128	242	209	bdl	0.91	1354	80.33	203.24	26.08	109.21	49.48	6.66	91.91	17.5	162.53	46.78	197.88	36.03	314.52	55.60
	2.5s	3855	146	240	452	bdl	1.58	1459	108.73	270.56	33.06	162.94	84.52	8.95	120.29	20.9	191.33	50.99	206.38	38.27	322.71	57.26
	5.0s	3763	107	216	773	0.84	1.02	1423	77.20	205.98	24.50	110.00	51.70	6.09	78.68	18.8	159.93	46.75	197.69	35.29	320.34	53.58
	7.5s	3779	88	204	388	bdl	1.35	1203	48.32	143.23	15.72	62.30	21.95	3.99	57.22	13.2	127.66	42.30	175.54	35.35	309.89	51.11
	10.0s	3808	54	156	232	0.71	bdl	777	38.29	73.59	10.13	31.43	12.36	2.19	27.10	7.0	80.00	26.02	109.7	22.65	197.12	37.13
	12.5s	3812	50	182	430	bdl	1.66	795	45.97	84.02	11.86	41.55	12.21	2.40	28.96	6.8	76.56	25.41	109.57	23.37	197.88	37.97
	15.0s	3812	50	184	685	0.96	bdl	799	53.50	94.24	11.06	45.57	11.44	1.73	30.25	6.4	81.91	26.18	109.01	22.17	196.74	36.09
	17.5s	3855	49	197	922	bdl	1.03	884	61.33	121.66	14.70	51.53	13.15	2.00	33.23	7.57	77.94	27.51	121.54	24.66	223.71	42.29
	20.0s	3737	39	101	341	bdl	0.55	614	64.01	107.77	14.17	52.91	12.06	2.60	22.42	6.38	64.99	17.33	82.82	16.10	149.91	26.33
	22.5s	3716	48	120	1006	1.01	1.23	702	76.24	137.65	17.87	57.94	19.90	2.38	26.90	7.28	65.58	22.14	93.66	18.51	170.29	31.47
	25.0s	3746	50	128	464	bdl	1.11	687	83.90	159.54	21.35	72.63	16.17	3.22	32.72	7.67	75.02	22.22	101.56	18.85	171.56	33.07
	27.5s	3720	39	105	354	3.56	1.22	621	99.40	173.02	23.02	82.36	16.81	2.08	34.76	6.52	60.97	19.37	74.48	17.21	154.03	28.03
	30.0s	3824	31	87	304	bdl	bdl	537	109.36	201.28	25.25	86.64	19.70	2.10	33.98	5.21	49.32	16.12	70.43	14.12	127.39	24.40
	32.5s	3690	28	90	700	bdl	0.63	481	100.80	182.69	25.32	74.41	18.86	2.92	27.62	5.18	44.02	14.19	59.31	12.05	120.14	21.57
	35.0s	3667	34	161	bdl	bdl	1.34	510	95.39	191.67	24.15	84.22	29.43	2.93	37.89	7.15	54.58	17.53	71.15	13.75	131.85	25.65
	37.5s	3511	30	230	679	2.77	1.30	534	93.76	190.67	25.67	84.69	30.54	3.80	40.04	6.74	54.53	18.11	70.22	17.16	166.77	31.32

Table 2 continued

Analysis	Site	Date[a]	Th	U	P	Ca	Sr	Y	La	Ce	Pr	Nd	Sm	Eu	Gd	Tb	Dy	Ho	Er	Tm	Yb	Lu
10C finish	40.0s (met)	3622	26	298	1883	bdl	2.41	667	81.68	151.61	19.92	77.90	20.02	2.66	34.93	6.75	56.99	19.07	98.71	23.48	233.04	42.53
ig (42–50s)		3848	125	250	491	bdl	0.73	1409	68.85	178.91	21.84	98.74	43.77	5.43	88.03	17.72	162.37	48.36	196.07	38.69	319.87	58.62
high LREE (36–39)		3836	434	434	759	bdl	1.49	2191	411.04	1005.14	111.97	610.07	294.91	26.62	435.31	60.24	356.01	79.35	234.03	41.70	336.53	55.66
16-1a	rim (met)	3626	45	172	886	bdl	0.84	835	49.08	94.76	12.12	41.11	10.75	0.71	22.45	6.56	79.81	27.09	117.68	23.37	189.54	29.77
16-1b	rim (met)	3622	43	184	771	bdl	0.23	836	bdl	2.14	0.03	0.71	2.33	0.11	15.86	6.19	79.20	27.42	119.92	23.84	191.31	29.85
16-2a	rim (met)	3598	67	253	868	bdl	0.47	1288	6.54	19.35	2.12	9.69	6.19	0.65	28.66	9.90	117.31	40.47	177.43	34.04	263.84	43.61
16-3a	rim (met)	3661	52	235	654	bdl	0.35	1038	0.85	4.35	0.13	1.80	2.97	0.16	20.12	7.48	99.54	33.99	146.64	29.11	233.41	37.85
9-1a	rim (met)	2577	4	347	221	bdl	0.44	337	1.87	5.05	0.68	2.17	1.70	0.19	5.53	1.22	18.90	8.78	56.02	16.30	183.88	45.39
G93/05 tonalite																						
3A	osc (ig)	3859	17	39	333	bdl	0.10	653	bdl	7.25	0.06	1.30	2.99	0.67	16.58	4.70	59.06	22.14	106.71	22.95	213.03	41.29
3B	osc (ig)	3808	25	36	290	bdl	0.08	895	0.01	7.08	0.20	4.41	7.25	1.59	35.48	9.17	99.69	31.76	132.10	25.81	224.39	39.42
3C	osc (ig)	3875	20	29	223	bdl	0.08	725	bdl	6.31	0.18	3.35	5.68	1.20	26.77	7.53	80.63	25.93	107.73	21.43	184.26	33.05
10A	osc (ig)	3840	55	74	432	bdl	0.13	1076	0.01	13.27	0.15	3.47	4.81	1.91	29.05	8.58	98.93	35.04	166.06	36.57	344.65	66.48
10B-s	osc (ig)	3808	86	127	288	bdl	0.10	776	0.02	15.28	0.08	1.76	3.18	0.73	21.76	6.26	73.14	26.47	121.91	26.60	245.19	46.53
10C	osc (ig)	3844	43	74	388	bdl	0.12	963	0.01	11.82	0.15	2.31	4.25	1.47	23.07	7.04	85.01	31.10	150.53	33.58	324.49	63.63
29A	osc (ig)	3658	21	55	231	bdl	0.15	375	0.02	5.75	0.05	1.15	2.09	0.48	11.11	3.11	35.86	12.67	58.52	12.86	121.55	23.27
29B	osc (ig)	3800	73	110	365	bdl	0.14	1033	0.03	16.59	0.13	2.97	5.29	1.12	28.62	8.85	101.81	34.92	162.20	33.52	309.74	56.41
29C	osc (ig)	3803	35	56	246	bdl	0.09	337	bdl	7.66	0.04	0.69	1.22	0.32	8.51	2.40	29.05	10.45	51.37	11.62	117.80	23.47
29D	osc (ig)	3800	17	51	158	bdl	0.06	191	bdl	5.31	0.01	0.36	0.66	0.18	3.98	1.20	15.18	5.68	29.67	7.17	76.63	16.10
22A	met	3598	22	325	324	bdl	0.04	123	bdl	0.88	0.02	0.97	2.83	0.34	18.84	4.17	24.89	3.93	10.01	1.56	12.62	2.28
22B	met	3598	35	299	323	bdl	0.04	69	bdl	1.12	0.05	1.40	3.76	0.33	22.89	4.50	21.42	2.18	3.16	0.37	1.90	0.28
G93/25 meta-quartzite from the Isua supracrustal belt																						
1A	det	3855	19	39	305	0.01	0.21	456	bdl	5.74	0.04	0.69	1.97	0.45	11.60	3.53	43.23	15.38	72.59	15.78	147.66	29.75
19A	det	3844	42	88	624	0.10	0.73	1026	0.63	9.24	0.39	3.50	4.30	1.16	23.09	7.51	92.50	34.35	158.73	32.94	300.85	57.37
20A	det	3820	87	177	337	bdl	0.48	1396	0.22	10.16	0.48	4.93	7.61	1.67	35.47	10.59	130.05	46.77	211.71	43.87	385.45	72.64
24A	det	3935	140	143	377	bdl	0.49	2116	0.10	19.15	0.51	8.41	14.92	3.16	78.34	20.61	226.48	74.35	314.27	61.10	525.78	95.24
17A	det	3901	125	234	506	0.07	0.70	1114	2.34	21.26	1.33	8.60	6.92	1.41	29.87	8.68	103.68	37.30	173.30	35.95	334.60	63.02
G97/92 inherited zircon in 3660 Ma granite south of the Isua supracrustal belt																						
3A	Inher	3750	30	128	347	0.0071	0.29	668	bdl	6.05	0.02	0.63	1.91	0.62	15.87	4.94	59.54	21.57	104.90	21.88	212.58	41.39
3B	Inher	3855	56	80	327	0.1977	0.30	1031	0.04	7.41	0.14	2.85	5.78	0.66	33.90	9.73	109.33	36.29	151.77	29.53	256.73	46.33

[a] Based on measured $^{207}Pb/^{206}Pb$—see text

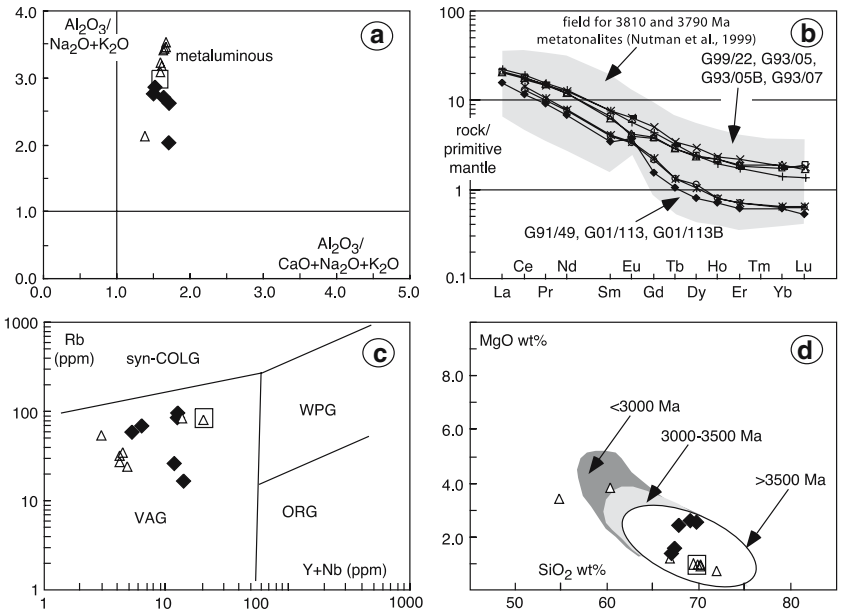

Fig. 8 Whole rock geochemistry. On frames **a**, **b** and **c** *filled diamonds* are ''best'' 3850 Ma samples, *open triangles* are c. 3795 and 3810 Ma Itsaq Gneiss Complex TTG (Nutman et al. 1999) and the *open square* is average value for >3500 Ma TTG from Martin et al. (2005). **a** $Al_2O_3/CaO + Na_2O + K_2O$ vs $Al_2O_3/Na_2O + K_2O$ plot demonstrating metaluminous character of 3850 Ma rocks. **b** Primitive mantle normalised REE plots (McDonough and Sun 1995). **c** Y + Nb vs Rb discrimination plot demonstrating Volcanic Arc Granite (VAG) character. **d** SiO_2 vs MgO plot showing that the 3850 Ma rocks plot in the field of >3500 Ma TTG of Martin et al. (2005)

(2005), the c. 3,850 Ma rocks plot in the >3,500 Ma fields predicted for their age (for example, SiO_2 vs. MgO; Fig. 8d).

^{147}Sm–^{143}Nd isotopic data for well-preserved 3,850 Ma rocks

Sm and Nd isotopic analyses (see data repository (see Electronic Supplementry Material) for the analytical method) were undertaken only on the five 3,850 Ma samples judged least modified based on field context and characteristics of the zircon populations (abundant oscillatory-zoned zircon and derived from single phase igneous protoliths). The Sm and Nd concentrations, measured isotopic compositions and calculated initial ε_{Nd}, values are presented in data repository in Table R4 of Electronic Supplementry Material and on Fig. 9. The initial ratios were calculated with reference to the presently accepted Sm–Nd reference parameters for CHUR (Jacobsen and Wasserburg 1980; Patchett et al. 2004). The error on the c. 3.85 Ga initial isotopic compositions is ≤ 0.5 epsilon units (2σ), and largely reflects the propagation of uncertainties associated with spike calibration and long-term reproducibility of standards, rather than in-run measurement precision, which is typically better than 10 ppm. The Nd concentrations are 8.70 to 40 ppm. The measured isotopic compositions ($\varepsilon_{Nd(0)}$ = –37 to –47) reflect the great age and LREE-enriched character of the gneisses. Four of the samples have initial compositions (calculated using the zircon age) overlapping within errors ($\varepsilon_{Nd(3.85)}$ = + 2.9 to +3.6) with one sample (G93/05) having a lower initial value of $\varepsilon_{Nd(3.85)}$ = + 0.6 (Fig. 9; Table 4).

The Eoarchaean destruction of c. 3,850 Ma quartzo–feldspathic rocks—migmatites, zircon xenocrysts and detrital grains

C. 3,850 Ma rocks that are almost homogeneous are extremely rare in the Itsaq Gneiss Complex. These are regarded as small domains that fortuitously survived the high strain, neosome production and pegmatite veining during polyphase Archaean tectonothermal events, which converted most of the Itsaq Gneiss Complex into banded multi-age component migmatites (McGregor 1973; Nutman et al. 1996, 2000, 2002). This section describes the migmatisation, which produced rocks of mixed age and origin, ultimately leading locally to c. 3,650 Ma granites sensu stricto that can carry older xenocrystic zircon. Also reviewed are the occurrences of c. 3,850 Ma detrital zircons in c. 3,806 Ma Isua sediments, interpreted to have been derived from erosion of 3,850 Ma rocks.

Table 3 Major and trace element compositions

Sample (field) Sample (ANU)	G91/49 92–369	G93/05 95–526	G93/05B	G99/22	G01/113	G01/113B	G93/07
SiO_2	69.04	67.65		66.92	69.59		67.29
Al_2O_3	15.52	16.03		16.09	15.54		15.55
Fe_2O_3	2.84	3.76		3.50	2.24		4.10
MnO	0.04	0.06		0.06	0.03		0.07
MgO	2.59	2.39		1.32	2.50		1.53
Cr_2O_3	0.00	0.00		0.01	0.01		0.02
TiO_2	0.31	0.41		0.51	0.27		0.49
CaO	5.82	4.53		4.61	4.38		4.45
K_2O	1.79	1.45		1.03	1.57		1.17
SO_3	0.01	0.02		<0.01	<0.01		0.01
P_2O_5	0.06	0.12		0.14	0.07		0.14
Na_2O	1.50	3.70		4.95	3.12		4.78
Total	99.54	100.15		99.80	99.83		99.61
Mg#	62.5	48.2		31.6	71.2		31.4
$CaO/(Na_2O+K_2O)$	1.77	0.88		0.77	0.93		0.75
Na_2O/K_2O	0.84	2.55		4.79	1.98		4.09
		Duplicate[a]			Duplicate[a]		
Sc	3.5	7.3	6.7	9.6	4.3	4.3	9.9
V	19	40	41	nd	nd	nd	nd
Co	31	11	10	6.7	4.3	4.5	30.9
Ni	34	43	42	31.0	30.8	37.1	26.0
Cu	10	5	4	8.5	21.5	19.6	nd
Zn	45	48	47	31.5	28.9	28.5	nd
Rb	58	94	81	16.5	66.7	66.7	25.1
Sr	123	128	126	350.4	96.0	93.7	337.7
Y	2.1	8.1	8.3	9.5	3.3	3.2	8.1
Zr	122	118	116	157.8	141.3	135.7	142.6
Nb	3.1	4.4	4.3	4.5	3.2	3.2	3.9
Cs	1.5	2.9	2.8	0.6	1.9	1.8	
Ba	97	90	87	93.5	120.7	120.3	115.2
La	10.1	13.4	13.9	nd	nd	nd	14.5
Ce	19.5	29.8	30.5	28.8	24.2	22.2	32.2
Pr	2.32	3.94	3.80	3.8	2.7	2.6	4.1
Nd	8.5	15.3	15.3	16.1	10.0	9.7	16.5
Sm	1.40	2.58	2.67	3.12	1.69	1.62	3.09
Eu	0.58	0.65	0.61	1.00	0.54	0.52	0.89
Gd	0.84	2.09	2.04	2.74	1.25	1.17	2.42
Tb	0.10	0.29	0.29	0.34	0.13	0.13	0.32
Dy	0.54	1.60	1.64	1.98	0.71	0.77	1.64
Ho	0.11	0.33	0.33	0.35	0.12	0.12	0.29
Er	0.27	0.83	0.81	0.96	0.31	0.31	0.75
Yb	0.27	0.84	0.78	0.82	0.29	0.28	0.63
Lu	0.036	0.11	0.13	0.12	0.044	0.043	0.093
Hf	3.50	3.29	3.07	4.13	3.79	3.65	3.38
Ta	0.52	0.30	0.29	0.30	0.27	0.26	
Pb	4.4	10.6	9.4	8.4	11.1	11.4	
Th	0.42	2.02	2.11	0.2	2.1	2.0	0.18
U	0.25	0.41	0.37	0.1	0.3	0.3	0.12

Table 3 continued

Sample (field)	G91/49	G93/05	G93/05B	G99/22	G01/113	G01/113B	G93/07
Sample (ANU)	92–369	95–526					
	1.66	5.18	4.77	5.03	1.75	1.71	3.88
Ce/Yb-n	19.2	9.4	10.4	9.3	22.6	21.1	13.5
La/Yb-n	26.0	11.0	12.4				15.8
Eu/Eu*	1.6	0.8	0.8	1.0	1.1	1.1	1.0
Sr/Y	58	16	15	37	30	30	42
Th/U	1.7	4.9	5.7	1.7	6.9	6.8	1.5
Zr/Hf	35.0	36.0	37.9	38.2	37.3	37.2	42.2

Major element data in wt%. Trace element data are in μg/g

[a] Duplicates represent separate powder aliquots and fusions

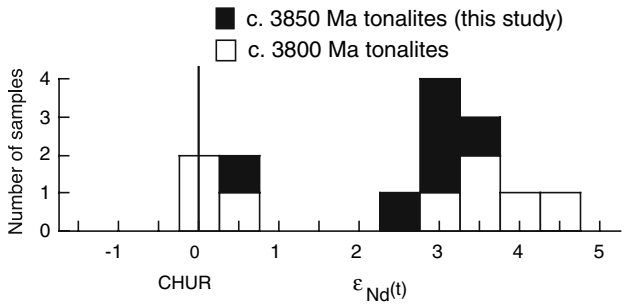

Fig. 9 Initial ε_{Nd} calculated at the crystallization age for 3850–3800 Ma felsic rocks Itsaq Gneiss Complex (includes data from Bennett et al. 1993). Only data for samples where there are independent age determinations by U–Pb zircon dating are included. The values for the c. 3850 Ma samples show a narrow range of positive ε_{Nd}

G93/07—representing rocks that are almost homogeneous but contain some in situ melt patches

The protolith characteristics of samples in this category are not as well preserved as G01/113 in terms of their degree of lithological homogeneity, and their zircons show a greater degree of recrystallisation. Zircon data for tonalite sample G93/07 with some nebulitic segregations are presented here. G93/07 is from a small island south of Akilia that is dominated by banded tonalitic gneisses. The sample locality (63°55.03′N, 51°40.89′W) is at the far top right of Fig. 5a, and the texture of the sampled rock is shown as an insert into the field photograph. Within the zone from which the sample was taken, the Ameralik dykes are strongly discordant and crosscut plutonic relationships in the Itsaq Gneiss Complex country rocks. The dominant lithology is meta-tonalite traversed by irregular felsic veins and nebulous patches, some of which contain blocky aggregates of hornblende (bottom of Fig. 5a) that from textural arguments (criteria in McGregor and Friend 1997) we interpret to be secondary after metamorphic orthopyroxene. Therefore these tonalites display the effects of high-grade migmatisation probably under granulite facies conditions, but because of the locally very low strain, the quantity of migmatisation veins and patches could be minimised (but not entirely excluded) when sampling. Because of unusually low strain, it is clear that tonalites represented by G93/07 intrude and break-up older mafic and ultramafic rocks (Fig. 5a).

G93/07 yielded prismatic to bipyramidal lilac zircons. In CL images the grains consist of interiors with strong

Table 4 Sm–Nd data for 3850 Ma gneisses

Sample	Age (Ga)	Nd (ppm)	Sm (ppm)	$^{147}Sm/^{144}Nd$	$^{143}Nd/^{144}Nd(0)$	±2 σ	$\varepsilon_{Nd}(0)$	$^{143}Nd/^{144}Nd(t)$	$\varepsilon_{Nd}(t)$[b]
G01/113A	3.844	8.7088	1.4393	0.0999	0.510328	9	–45.06	0.50778	3.0
G91-49[b]	3.858	10.7024	1.7078	0.0961	0.510214	9	–47.28	0.50778	2.9
G91-49[b]	3.858	15.5014	1.5109	0.0972	0.510209	8	–47.38	0.50775	2.4
G93/05	3.841	15.0515	2.7968	0.1124	0.510522	10	–41.28	0.50766	0.6
G99/22R	3.855	39.9960	7.6456	0.1155	0.510745	8	–36.93	0.50780	3.6
G93/07	3.852	15.6972	2.9779	0.1146	0.510704	8	–37.73	0.50778	3.2

Nd isotopic compositions normalised to $^{146}Nd/^{144}Nd = 0.7219$

[a] Data reported in Bennett et al. 1993 (sample listed as 92-369) from two separate powder aliquots

[b] Error based on all uncertainties including spike calibrations estimated to be <±0.5 epsilon units

oscillatory-zoning, and with mantles of generally brighter (lower U) zircon that are weakly zoned to homogeneous (data repository for CL images in Fig. R2a of Electronic Supplementry Material). Some grains are dominated by 3,850 Ma zircon with strong oscillatory-zoning, with only an incomplete mantle of younger zircon present. In other grains outer mantles are more volumetrically dominant (e.g. grain 3), and in some cases are clearly formed by replacement of the zoned interior (e.g. grain 9, data repository in Fig. R2a of Electronic Supplementry Material). The strongly zoned zircons yielded close to concordant dates (Table 1, Fig. 6b), with a weighted mean $^{207}Pb/^{206}Pb$ date of 3,852 ± 12 Ma (MSWD = 0.93). Mantles of less strongly zoned to homogeneous zircon yielded younger ages and lower Th/U. These were not examined in as much detail with SHRIMP as the strongly zoned zircon, but from the available data, it would appear that 3,740–3,700 and 3,650–3,600 Ma zircon are present. Our preferred interpretation of these results is that tonalite G93/07 is c. 3,850 Ma old, but that during later Eoarchaean metamorphic events and development of nebulitic patches in the rock, zircon was subjected to recrystallisation and regrowth.

Migmatites and inheritance-bearing neosome

Sample G88/66 is a banded migmatitic gneiss from southwestern Akilia (see Fig. 9a of Nutman et al. 2000), and was the first proposed (albeit poorly preserved) c. 3,850 Ma rock in Greenland. In our interpretation, this gneiss contains a c. 3,850 Ma component, but has been overprinted at c. 3,660 Ma by development of neosome and/or veining and then strongly deformed and metamorphosed several times until late in the Archaean (Nutman 1990; Nutman et al. 1996, 2000; Friend and Nutman 2005a). Here, data on three additional banded gneiss samples are presented: G01/109 is a quartz diorite (Table 1) with sparse veins deformed into a banding. VM95/02 and G05/39 are strongly deformed, polyphase, banded migmatites rich in neosome and palaeosome, respectively. G01/109 comes from the same island c. 1 km west of Akilia that yielded sample G01/113. It was collected at (63°55.83′N, 51°43.85′W) from a c. 5 m wide tract of gneiss that contains inclusions of amphibolite and (clinopyroxene-rich) skarn (Fig. 5b), suggesting that its igneous protolith was intruded into a mafic supracrustal(?) host. G01/109 is well foliated and is heterogeneous due to felsic segregations and mafic schlieren.

G01/109 gave a small yield of lilac-coloured zircons. About 90% of the grains are prismatic in habit, with the remaining being equant. CL imaging shows that the prismatic grains have oscillatory zoning parallel to the grain exteriors, but that the zoning has been widely disrupted by discordant recrystallisation domains (data repository in Fig. R2b of Electronic Supplementry Material). Most grains have skins of less-zoned zircon, ranging from a few microns on prismatic faces to more on pyramidal ones. Equant grains have internal structure dominated by sector zoning. Twenty-eight SHRIMP U–Pb analyses were undertaken on 18 grains and all yielded close to concordant ages. Of these, 19 were analyses of oscillatory-zoned zircon that yielded $^{207}Pb/^{206}Pb$ dates between c. 3,850 and 3,600 Ma (Table 1; Fig. 6c). Three analyses in grain 5 of oscillatory-zoned zircon displayed the same age spread. Therefore, we interpret the zoned zircon as having a single age, but to have been variably disturbed through some loss of radiogenic Pb in the Eoarchaean. Using this interpretation, seven analyses with the highest $^{207}Pb/^{206}Pb$ dates yield a weighted mean age of 3,829±10 Ma (95% confidence, MSWD = 0.52). This is taken as the best estimate of the minimum protolith age of G01/109. Two rim analyses on prismatic grain 8 gave indistinguishable $^{207}Pb/^{206}Pb$ dates at c. 3,650 Ma, whereas all seven analyses of equant sector-zoned zircons gave a weighted mean $^{207}Pb/^{206}Pb$ date of 3,619±16 Ma (95% confidence, MSWD = 1.5). The disturbance of U/Pb data from oscillatory-zoned zircon grains, coupled with CL images, indicates recrystallisation and new zircon growth in Eoarchaean tectonothermal events.

In the fjord Itilleq and on the semi-nunatak Ivisaartoq (Fig. 1), reconnaissance geological mapping has long recognised the presence of Eoarchaean gneisses (Allaart et al. 1977; Hall and Friend 1979). These have been scientifically neglected compared with the gneisses of Akilia and surrounding islands in the southwest, and the Isua area in the north. The banded gneiss sample (VM95/02), as the first reconnaissance zircon dating samples from Itilleq, was deliberately collected (by the late V. R. McGregor) in contact with an Ameralik dyke, in order to give the clearest possible field setting (Fig. 5c). The banded gneiss sample contains a large amount of strongly deformed neosome, and indicates that an older component was either subjected to in situ incipient partial melting or was veined by granitic material, prior to strong deformation that transformed it into banded gneiss.

In keeping with the migmatitic nature of the rocks, VM95/02 zircons are structurally complex (e.g. data repository in CL images in Fig. R2c of Electronic Supplementry Material). CL imaging shows that oscillatory-zoned cores and rims are present in some grains, whereas in other grains only one generation of oscillatory-zoned zircon is present. Discordant recrystallisation domains that appear homogeneous in CL images disrupt oscillatory zoning. In addition some outermost (partial) rims that appear homogeneous in CL images are present.

Twenty-four SHRIMP U/Pb analyses were undertaken on 17 zircons (Table 1). Seventeen analyses yielded slightly discordant ages, whereas only seven are concor-

dant (Fig. 6d). In addition some have strongly discordant ages and are not considered here. Two cores identified in the CL imaging, have $^{207}Pb/^{206}Pb$ dates of >3,800 Ma (grain 4, data repository in Fig. R2c of Electronic Supplementry Material). Most analyses from grains with only a single generation of oscillatory-zoned zircon (grain 6, data repository in Fig. R2c of Electronic Supplementry Material), or from oscillatory-zoned rims in composite grains, yield a bimodal distribution of $^{207}Pb/^{206}Pb$ ages with ''peaks'' at c. 3,665 Ma and 3,625 Ma. Thus the sample contains two, or perhaps three, generations of oscillatory-zoned zircon, in keeping with the interpretation in the field of this as a composite gneiss with some palaeosome (>3,800 Ma) in more abundant neosome (3,660–3,600 Ma).

Banded gneiss sample G05/39 from Ivisaartoq (Fig. 1) also yielded complex zircons like VM95/02, with oscillatory-zoned zircon forming the interior of grains. Grain exteriors consist of homogeneous to sector-zoned domains that appear brighter in CL images (lower U + Th). Most analyses gave close to concordant ages (Table 1; Fig. 6e). Analyses on the oscillatory-zoned zircon yielded ages mostly >3,800 Ma. Repeat analyses on single grains indicated that spread in $^{207}Pb/^{206}Pb$ dates is due to variable Pb loss. Using an interpretation of variable amounts of ancient loss of radiogenic Pb from a single >3,800 Ma population applied to other samples, those analyses with the oldest apparent $^{207}Pb/^{206}Pb$ dates yielded ages of c. 3,850 Ma. This is interpreted as the age of the palaeosome in this sample. Analyses of the homogeneous to sector-zoned grain exteriors yielded younger ages of mostly 3,660–3,600 Ma. In addition, a minority of oscillatory-zoned zircons (site 4.1, Table 1, repository, Fig. R2d) also yielded these young ages. These are interpreted to date as high-grade metamorphism, associated with neosome development and partial melting between 3,660 and 3,600 Ma.

To assess further the age profile of migmatite components within the Itsaq Gneiss Complex, reconnaissance zircon dating of samples is being undertaken from localities scattered across the parts of the complex where formerly there was little or no geochronological data (Fig. 1; Table 1). In this reconnaissance programme that still continues (ultimately 80 more samples will be dated), analyses are undertaken mostly on the Hiroshima SHRIMP II instrument, with a lesser number having been performed on the ANU SHRIMP RG instrument. Analysis focuses on oscillatory-zoned zircon forming the interior of grains, with a lesser number of analyses being undertaken on the more homogeneous exterior domains of the grains. The amount of oscillatory-zoned zircon varies considerably between samples. In some it is the dominant component, with only thin mantles of younger zircon, whereas in other it was restricted to volumetrically much smaller cores. Only the five reconnaissance samples so far where c. 3,850 Ma (shorthand for 3,840–3,880 Ma) zircons were encountered are presented in this study (Table 1, Figs. 1, 6f). The discovery of c. 3,850 Ma components in migmatites at several new localities shows that this component is a widespread, but probably a volumetrically minor, component in the Itsaq Gneiss Complex.

Trace element geochemistry of c. 3,850 Ma inherited zircon in granites and 3,850 Ma detrital grains in metasediments

LA- ICP-MS trace element analyses of four c. 3,850 Ma and one 3,900 Ma detrital zircon in meta-quartzite G93/25 (Nutman et al. 1997b) and two analyses of a c. 3,850 Ma inherited zircon core in 3,660 Ma granite G97/92 (Friend and Nutman 2005a) have been undertaken. The data are presented in Table 2 and are summarised in Fig. 10. CL images (unpublished) of G93/25 detrital zircons show they are homogeneous or display oscillatory zoning. They have heavy REE at 1,000–3,000 × chondritic abundances, with minor negative Eu anomalies, positive Ce anomalies and strong depletion of the other light REE. The 3,900 Ma grain (grain 17, Nutman et al. 1997b) found in this metasediment is the oldest zircon yet published from the Itsaq Gneiss Complex. It has similar but slightly more LREE-enriched patterns compared to the c. 3,850 Ma zircons

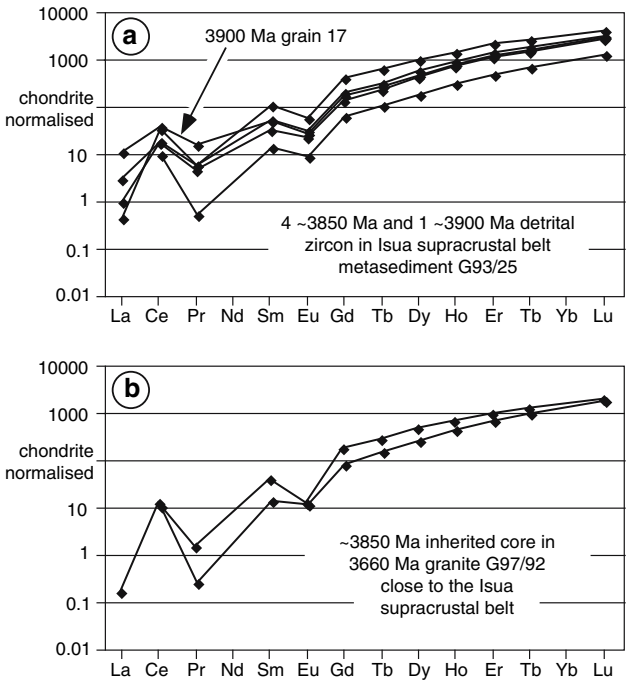

Fig. 10 Laser ablation ICP-MS chondrite-normalised REE analyses for **a** detrital grains from metaquartzite G93/25 and **b** inherited 3850 Ma zircon core in 3660 Ma granite G97/92

from the metasediment. Likewise the c. 3,850 Ma inherited core in 3,660 Ma granite G97/92 igneous zircons shows similar REE patterns and abundances. This suggests crystallisation of these c. 3,850 Ma zircons in the presence of plagioclase (negative Eu anomalies) and the absence of garnet (elevated heavy REE abundances). These are typical REE patterns and abundances for zircons crystallised in granitic (sensu lato) magmas and indicate that in the Eoarchaean, erosion and intra-crustal partial melting were already destroying some 3,900 to 3,850 Ma sialic crust.

Discussion

Nature and extent of the c. 3,850 Ma geological record in the Itsaq Gneiss Complex

All Eoarchaean rocks (>3,600 Ma) are contained in gneiss terrains, where they are intruded by younger granitoids, and all have undergone variable but generally strong polyphase ductile deformation under amphibolite or granulite facies metamorphic conditions, leading to variable degrees of in situ migmatisation. Thus >95% of the quartzo–feldspathic rocks in the (≈3,000 km^2) Itsaq Gneiss Complex are banded gneisses of little use for detailed modern isotopic and geochemical investigations concerning the accretion and differentiation of the oldest juvenile crust. The other <5% of the Complex, containing the less deformed and migmatised rocks that are suitable for such investigations, is largely in the Complex's northern end and consists of 3,810, 3,790, 3,700 Ma tonalites and c. 3,650 Ma granites (Nutman et al. 1996, 1999, 2000; Crowley et al. 2002; Crowley 2003). In contrast, the presently *known* amount of well preserved c. 3,850 Ma quartzo–feldspathic rock is much smaller and occurs in a few small domains of coinciding lower strain and less severe 3,660–3,600 Ma migmatisation (Nutman et al. 2000; 2002a; this study). These provide a unique window back to the early Earth at 3,850 Ma, pre—the formation of the Isua supracrustal rocks. Thus the ''best'' 3,850 Ma metatonalite G01/113 retains its integrity (free of veining and in situ neosome) for only a few m^2 of the outcrop (Fig. 3).

Integrated field and zircon studies reported here have tracked the fate of such c. 3,850 Ma tonalites during superimposed tectonothermal events, and here we propose that they are transformed into palaeosome components distributed within migmatites strongly affected by pegmatite veining and in situ melting between 3,660 and 3,600 Ma. As a continuation to the in situ melting and migmatisation, low temperature crustally derived granites in the Itsaq Gneiss Complex can carry inherited older zircon (e.g., grain 3 in 3,661 Ma granite G97/92 dated by Friend and Nutman 2005a). Furthermore, c. 3,850 Ma detrital zircons are present in rare clastic metasediments in the Itsaq Gneiss Complex (Nutman et al. 1997b). Thus field and zircon data indicate that c. 3,850 Ma quartzo–feldspathic rocks are a widespread, but probably now a volumetrically minor, component of the Itsaq Gneiss Complex.

Interpreting Nd isotopic data from 3,850 to 3,600 Ma Itsaq Gneiss Complex rocks

The Nd compositions presented here provide some of the oldest direct constraints on Nd mantle compositions, with only samples of the Acasta gneisses from the Slave Province of Northwest Canada, being older at 3,900–4,000 Ma (Bowring et al. 1989; Bowring and Housh 1995). The new data fall within the same range, but with a narrower spread of compositions than previously presented for >3,700 Ma rocks from the Itsaq Gneiss Complex (Bennett et al. 1993; Jacobsen and Dymek 1988) (Fig. 10). The greater homogeneity apparent in the more recent data set may at least partly reflect more stringent selection criteria than previously employed. It is likely that some earlier data, for example the widely studied banded gneiss sample 110999 (collected in the early 1970s) with $\varepsilon_{Nd(3.82\ Ga)} = +0.1$ and for 90–532, the single sample of Bennett et al. (1993) with an apparent negative initial ε_{Nd}, may reflect the effects of mixing of two or more gneiss components (Nutman et al. 2004b), although further work is necessary for verification. The data set for the 16 samples of >3,700 Ma gneisses (with the one exception of sample 90–532), including the data for the 3,850 Ma gneisses presented here, have a limited range of initial compositions, from 0 to +4.5. There is no evidence for the degree of mantle heterogeneity suggested by Nd isotope data from the slightly older Acasta gneisses (Bowring and Housh 1995) with apparent initial ε_{Nd} (4.0 Ga) from +3.5 to –4.8. The lack of negative ε_{Nd} values in the tonalites of the Itsaq Gneiss Complex is complementary with the absence of much older zircons in the Complex and with the lack of negative initial ε_{Hf} (e.g. Vervoort et al. 1996) in them. On the other hand, the Acasta gneisses contain rare, significantly older Hadean zircon xenocrysts (Iizuka et al. 2006). All of these observations indicate that there was not a widespread significantly older (>3,850 Ma) felsic component in the sources of the Itsaq Gneiss Complex samples.

The uniformity of the isotopic data obtained from the c. 3,850 Ma suite (apart from G93/05), in terms of both initial ε_{Nd} values and narrow range of measured $^{147}Sm/^{144}Nd$, shows the likely consanguineous nature of these rocks. There are several possible explanations for the lower ε_{Nd}

value of G93/05. First and foremost, the slightly lower ε_{Nd} of this sample as compared to the other four tonalites, may accurately reflect the source composition of the rock and indicates some mantle heterogeneity i.e. that the mantle source of this sample was less LREE depleted than that of the other samples. Other possibilities suggested may arise from misinterpretation of the age data. Assuming that the rock is only c. 3,650 Ma old, with nearly all its zircon inherited, as suggested by Whitehouse and Kamber (2005), will result in the calculation of a spurious ε_{Nd} value at 3,850 Ma. Another possibility, using our interpretation that this rock is c. 3,850 Ma old, is that G93/05 was derived entirely, or at least in part, by melting of a LREE-enriched protolith appreciably older than 3,850 Ma. This would be a hint that some extremely ancient (>4,000 Ma) crust might have been present when some of the oldest parts of the Itsaq Gneiss Complex were formed. Finally, despite the most careful sample screening, if there was minor alteration of the Sm/Nd ratio during superimposed tectonothermal events, the calculated initial ε_{Nd} of this rock could be inaccurate. Nonetheless, there is much greater uniformity in our Nd isotopic data set than that obtained on polyphase migmatites such as the Acasta gneisses (Bowring and Housh 1995; Moorbath et al. 1997). Dispersion in the initial ε_{Nd} values for Acasta gneisses may be due either to secondary Sm/Nd disturbance during younger superimposed tectonothermal events, or because several protolith components of different age and isotopic signatures (including some >4.0 Ga crust—Iizuka et al. 2006) are present in the samples. Clearly, working on well-preserved sets of rocks, such as our ''best'' tonalites preserved here, generate isotopic data that are more concise and readily interpretable than data obtained from polyphase migmatites.

Depletion history of the pre-3,850 Ma mantle from ^{147}Sm–^{143}Nd isotope systematics

Initial Nd isotopic compositions reflect the time-integrated Sm/Nd ratio of the gneiss source(s) that in turn reflects the average degree of lithophile element depletion or enrichment. The degree of the depletion of the mantle in the first billion years of Earth history as recorded in the initial $^{143}Nd/^{144}Nd$ compositions of the oldest rocks has long been recognised as a key constraint for models of the early differentiation of the Earth (e.g. Jacobsen and Wasserburg 1979; Galer and Goldstein 1991). Owing to the significance of the results for interpreting early Earth history, there has been much controversy and debate over the meaning of the data from the oldest rocks. Earlier aspects of this debate centred on uncertainties in the crystallisation ages used to calculate initial compositions, have now been largely eliminated through the use of modern dating methods, primarily ion microprobe U–Pb dating of single zircons combined with the use of CL imagery. The controversy has focussed more recently on the veracity of calculated initial compositions because of the potential of secondary resetting of isotopic systems including Sm–Nd (e.g. Gruau et al. 1996). An additional aspect when using felsic rocks to determine mantle compositions is that, in general, granitoids in any tectonic setting have a range of initial isotopic compositions reflecting the complexity of granite-forming processes. For example, Phanerozoic batholiths (e.g. Sierra Nevada Batholith) that have not experienced deformation or metamorphism, and have well-defined ages, show a range in ε_{Nd}, from near-depleted mantle values to those of the compositions of the oldest crust in the area (DePaolo 1981). The samples with the most positive ε_{Nd} values are generally taken as most representative of the mantle, but the less positive values are not in error, but reflect a mixture of source materials.

Although much has been said about the potential role of secondary Sm/Nd modification leading to the calculation of erroneous initial compositions, recent studies suggest that careful sample selection can minimise these effects. For example, Baxter and DePaolo (2004) demonstrated that even during severe metamorphism mobility of Sm and Nd in solid systems is only on the centimetre scale. Thus single-phase gneisses, such as the ''best'' samples that we have presented in this paper, should be able to preserve Sm–Nd systematics, when sampled and prepared carefully. Therefore we are confident that the ^{143}Nd database for the oldest, single-component, homogeneous felsic samples provides strong evidence for strong early differentiation of the pre-3,850 Ma mantle.

As has been discussed in numerous papers (e.g. Bennett et al. 1993; Caro et al. 2003), that generating $\varepsilon_{Nd} = +3$ before 3,850 Ma in the upper mantle source of the ancient tonalites requires rapid early depletion (increase in Sm/Nd). Mechanisms suggested to create a high Sm/Nd upper mantle in the early Earth include production of voluminous quantities of early continental crust (first proposed by Armstrong 1981 and more recently advocated by Bowring and Housh 1995 and Harrison et al. 2005), early formation of a LREE-enriched basaltic crust (Chase and Patchett 1988) and formation of early, deep mantle reservoirs (e.g. Tolstikin and Hofmann 2005). Additional support for deep reservoir models comes from recent ^{142}Nd results showing apparent distinctions between the Earth and chondrites (Boyet and Carlson 2005) implying rapid early global Earth differentiation.

Country rocks to c. 3,850 Ma tonalites

Tonalites do not represent primary crust produced by directly melting the mantle. Instead, they are secondary

crust, and are mostly considered to be produced by melting of hydrated mafic crustal rocks in the stability field of garnet (Martin et al. 2005 and references therein). Therefore the 3,850 Ma tonalites described here must have been intruded into older crustal rocks. The most common host for tonalites throughout the Archaean geological record of the whole world are mafic rocks, derived largely from meta-basalts with some gabbros (McGregor 1973 onwards). In accordance with this, Nutman et al. (1997a, 2000, 2002, this study) have presented field evidence (discordant relationships) at localities, including Akilia, that indicate c. 3,850 Ma tonalites were intruded into older mafic rocks, with rare layers of silica- and iron-rich rocks (Fig. 4; Nutman et al. 1997, 2000, 2002). On Akilia these silica- and iron-rich rocks display an iron isotopic signature (Dauphas et al. 2004) and trace element spectra identical to that observed in Isua supracrustal belt banded iron formations (Friend et al. 2007). Thus in our interpretation, the Itsaq Gneiss Complex contains rare ≥ 3,850 Ma mafic and sedimentary rocks that are older than those in the Isua supracrustal belt, and hence the oldest known on Earth. However, it should be noted that others contest this interpretation (e.g. Whitehouse and Kamber 2005).

Conclusions

(1) The state of preservation of 3,850 Ma quartzo–feldspathic rocks ranges from geochemically modified palaeosome within polyphase migmatites to near-homogeneous tonalites and quartz-diorites. A few samples of the latter are the best candidates to examine the formation of the oldest portions of quartzo–feldspathic crust in Greenland by whole rock geochemistry and Nd isotopes. We consider that tonalite G01/113 is presently the world's best-preserved ''pre-Isua'' (i.e. pre- 3,710 and 3,810 Ma) rock. The only known older terrestrial quartzo–feldspathic rocks are rare migmatite components in the Acasta Gneisses (Bowring et al. 1989; Bowring and Williams 1999) and at Mt Sones in Antarctica (Black et al. 1986).

(2) Detrital 3,850 Ma zircons in rare clastic metasediments from the Isua supracrustal belt display negative Eu anomalies in their chondrite-normalised REE patterns, with the heavy REE showing chondrite-normalised values of c. 1,000. Combined with the oscillatory zoning displayed by some of these zircons, it is likely that they were derived from c. 3,850 Ma quartzo–feldspathic igneous rocks that were destroyed by Eoarchaean erosion.

(3) The quantity of c. 3,850 Ma quartzo–feldspathic crust detected in the Itsaq Gneiss Complex, on the basis of present information, is volumetrically much less than the 3,810–3,790, 3,760–3,740 and 3,700–3,690 Ma tonalite suites.

(4) Initial ε_{Nd} values determined from the five best preserved 3,850 Ma rocks demonstrate a narrow range of compositions. These data provide strong evidence for a mantle value of $\varepsilon_{Nd} = +3$ at 3,850 Ma and strengthen arguments for rapid early depletion of at least portions of the upper mantle (e.g. Bennett et al. 1993; Caro et al. 2003). The major and trace element compositions of these tonalites are similar to other Archaean TTG suites both in West Greenland (Nutman et al. 1999) and worldwide (e.g. Martin et al. 2005) indicating continuity of TTG crust formation processes throughout the Archaean

Acknowledgments The contributions of the late Vic R. McGregor to the early phases of this work are gratefully acknowledged. Shane Paxton and Jon Mya are thanked for heavy mineral separations. Charlotte Allen is thanked for assistance with LA-ICP-MS analyses. We acknowledge support from ARC grant DP0342794 and NERC Grant GR3/13039. Ole Christiansen of Nunaminerals A/S is thanked for logistic assistance in Greenland. The manuscript was considerably improved with the advice from the two reviewers Nigel Kelly and Balz Kamber and the handling editor Ian Parsons.

References

Allaart JH (1976) The pre-3760 m.y. old supracrustal rocks of the Isua area, central West Greenland, and the associated occurrence of quartz-banded ironstone. In: Windley BF (ed) The early history of the Earth. Wiley, London, pp 177–189

Allaart JH, Jensen SB, McGregor, VR, Walton BJ (1977) Reconnaissance mapping for the 1:500,000 map sheet in the Godthåb-Isua region, southern West Greenland. Rapport Grønlands Geologiske Undersøgelse 85:50–54

Armstrong RL (1981) Radiogenic isotopes: The case for recycling on a near steady state, no continental growth Earth. Phil Trans Royal Soc London A301:443–472

Baadsgaard H (1973) U–Th–Pb dates on zircons from the early Precambrian Amîtsoq gneisses, Godthaab district, West Greenland. Earth Planet Sci Lett 19:22–28

Baadsgaard H, Nutman AP, Bridgwater D (1986) Geochronology and isotopic variation of the early Archaean Amîtsoq gneisses of the Isukasia area, southern West Greenland. Geochim Cosmochim Acta 50:2173–2183

Baxter EF, DePaolo DJ (2004) Can metamorphic reactions proceed faster than bulk strain? Contrib Mineral Petrol 146:657–670

Bennett VC, Nutman AP, McCulloch MT (1993) Nd isotopic evidence for transient, highly depleted mantle reservoirs in the early history of the Earth. Earth Planet Sci Lett 119:299–317

Bennett VC, Nutman AP, Esat TM (2002) Constraints on mantle evolution and differentiation from $^{187}Os/^{188}Os$ isotopic compositions of Archaean ultramafic rocks from southern West Greenland (3.8 Ga) and Western Australia (3.45 Ga). Geochim Cosmochim Acta 66:2615–2630

Black LP, Gale NH, Moorbath S, Pankhurst RJ, McGregor VR (1971) Isotopic dating of very early Precambrian amphibolite facies gneisses from the Godthåb district, West Greenland. Earth Planet Sci Lett 12:245–259

Black LP, Williams IS, Compston W (1986) Four zircon ages from one rock; the history of a 3930 Ma-old granulite from Mount Sones, Enderby Land, Antarctica. Contrib Mineral Petrol 94:427–437

Bowring SA, Housh TB (1995) The Earth's early evolution. Science 269:1535–1540

Bowring SA, Williams IS (1999) Priscoan (4.00–4.03 Ga) orthogneisses from northwestern Canada. Contrib Mineral Petrol 134:3–16

Bowring SA, Willams IS, Compston W (1989) 3.96 Ga gneisses from the Slave province, Northwest Territories, Canada. Geology 17:760–764

Boyet M, Carlson RW, (2005) ^{142}Nd evidence for early (>4.53 Ga) global differentiation of the silicate Earth. Science 309:576–561

Bridgwater D, McGregor VR (1974) Field work on the very early Precambrian rocks of the Isua area, southern West Greenland. Rapport Grønlands geologiske Undersøgelse 65:49–54

Bridgwater D, Keto L, McGregor VR, Myers JS (1976) Archaean gneiss complex of Greenland. In: Escher A, Watt WS (eds) Geology of Greenland. Geological Survey of Denmark and Greenland, Copenhagen, pp 18–75

Caro G, Bourdon B, Birk J-L, Moorbath S (2003) ^{146}Sm–^{142}Nd evidence from Isua metamorphosed sediments for early differentiation of Earth's mantle. Nature 423:428–432

Chadwick B (1981) Field relations, petrography and geochemistry of Archaean amphibolite dykes and Malene supracrustal amphibolites, northwest Buksefjorden, southern West Greenland. Precamb Res 14:221–259

Chadwick B, Nutman AP (1979) Archaean structural evolution in the northwest of the Buksefjorden region, southern West Greenland. Precamb Res 9:199–226

Chase CG, Patchett PJ (1988) Stored mafic/ultramafic crust and early Archean mantle depletion. Earth Planet Sci Lett 91:66–72

Collerson KD, Bridgwater D (1979) Metamorphic development of early Archaean tonalitic and trondhjemitic gneisses: Saglek area, Labrador. In: Barker F (ed) Trondhjemites, dacites and related rocks. Elsevier, Amsterdam, pp 659

Crowley JL (2002) Testing the model of late Archean terrane accretion in southern West Greenland: a comparison of the timing of geological events across the Qarliit nunaat fault, Buksefjorden region. Precambrian Res 116:57–79

Crowley JL (2003) U–Pb geochronology of 3810–3630 Ma granitoid rocks south of the Isua greenstone belt, southern West Greenland. Precamb Res 126:235–257

Crowley JL, Myers JS, Dunning, GR (2002) The timing and nature of multiple 3700–3600 Ma tectonic events in granitoid rocks north of the Isua greenstone belt, southern West Greenland. Geol Soc Am Bull 114:1311–1325

Dauphas N, van Zuilen M, Wadhwa M, Davis AM, Marty B, Janney PE (2004) Clues from Fe isotope variations on the origin of early Archean BIFs from Greenland. Science 306:2077–2080

DePaolo DJ (1981) A neodymium and strontium isotopic study of the Mesozoic calc-alkaline granitic batholiths of the Sierra Nevada and Peninsular Ranges, California. J Geophys Res 86:10470–10488

Frei R, Polat A (2007) Source heterogeneity for the major components of ~3.7 Ga banded iron formation (Isua Greenstone Belt, Western Greenland): tracing the nature of interacting water masses in BIF formation. Earth Planet Sci Lett 253:266–281

Friend CRL, Nutman AP (2005a) Complex 3670–3500 Ma orogenic episodes superimposed on juvenile crust accreted between 3850 and 3690 Ma, Itsaq Gneiss Complex, southern West Greenland. J Geol 113:375–397

Friend CRL, Nutman AP (2005b) New pieces to the Archaean terrane jigsaw puzzle in the Nuuk region, southern West Greenland: steps in transforming a simple insight into a complex regional tectonothermal model. J Geol Soc Lond 162:147–162

Friend CRL, Nutman AP, Bennett VC, Norman MD (2007) Early terrestrial seawater signature from a >3850 Ma (earliest life?) sediment from Akilia, southern West Greenland. Contrib Mineral Petrol. (considered suitable for publication pending major revisions, 14 November 2006) (in press)

Friend CRL, Nutman AP, McGregor VR (1987) Late-Archaean tectonics in the Færingehavn–Tre Brødre area, south of Buksefjorden, southern West Greenland. J Geol Soc Lond 144:369–376

Friend CRL, Nutman AP, McGregor VR (1988) Late Archaean terrane accretion in the Godthåb region, southern West Greenland. Nature 335:535–538

Friend CRL, Nutman AP, Baadsgaard H, Kinny PD, McGregor VR (1996) Timing of late Archaean terrane assembly, crustal thickening and granite emplacement in the Nuuk region, southern West Greenland. Earth Planet Sci Lett 124:353–365

Friend CRL, Bennett VC, Nutman AP (2002) Abyssal peridotites >3800 Ma from southern West Greenland: field relationships, petrography, geochronology, whole-rock and mineral chemistry of dunite and harzburgite inclusions in the Itsaq Gneiss Complex. Contrib Mineral Petrol 143:71–92

Galer SJG, Goldstein SL (1991) Early mantle differentiation and its thermal consequences. Geochim Cosmochim Acta 55:227–239

Gill RCO, Bridgwater D (1979) Early Archaean basic magmatism in West Greenland: the geochemistry of the Ameralik dykes. J Pet 20:695–726

Griffin WL, McGregor VR, Nutman AP, Taylor PN, Bridgwater D (1980) Early Archaean granulite facies metamorphism south of Ameralik. Earth Planet Sci Lett 50:59–74

Gruau G, Rosing M, Bridgwater D, Gill RCO (1996) Resetting of Sm–Nd systematics during metamorphism of >3.7 Ga rocks; implications for isotopic models of early Earth differentiation. Chem Geol 133:225–240

Hall RP, Friend CRL (1979) Structural evolution of the Archean rocks in Ivisârtoq and the neighbouring inner Godthåbsfjord region, southern West Greenland. Geology 7:311–315

Harrison TM, Blichert-Toft J, Muller W, Albarede F, Holden P, Mojzsis SG (2005) Heterogeneous Hadean hafnium: evidence of continental crust at 4.4 to 4.5 Ga. Science 310:1947–1950

Iizuka T, Horie K, Komiya T, Maruyama S, Hirata T, Hidaka H, Windley BF (2006) 4.2 Ga zircon xenocryst in an Acasta gneiss from northwestern Canada: evidence for early continental crust. Geology 34:245–248

Jacobsen SB, Dymek RF (1988) Nd and Sr isotope systematics of clastic metasediments from Isua, West Greenland: identification of pre-3.8 Ga differentiated crustal components. J Geophys Res 93:338–354

Jacobsen SB, Wasserburg GJ (1979) The mean age of mantle and crustal reservoirs. J Geophys Res 84:7411–7427

Jacobsen SB, Wasserburg GJ (1980) Sm–Nd isotopic evolution of chondrites. Earth Planet Sci Lett 50:139–155

Kamber BS, Moorbath S (1998) Initial Pb of the Amîtsoq gneiss revisited: implication for the timing of early crustal evolution in West Greenland. Chem Geol 150:19–41

Kamber BS, Collerson KD, Moorbath S, Whitehouse MJ (2003) Inheritance of early Archaean Pb-isotope variability from long-lived Hadean protocrust. Contrib Mineral Petrol 145:25–46

Kinny PD (1986) 3820 Ma zircons from a tonalitic Amîtsoq gneiss in the Godthåb District of southern West Greenland. Earth Planet Sci Lett 79:337–347

Kinny PD, Nutman AP (1996) Zirconology of the Meeberrie gneiss, Yilgarn Craton, Western Australia: an early Archaean migmatite. Precamb Res 78:165–178

Komiya T, Maruyama S, Masuda T, Appel PWU, Nohda S (1999) The 3.8–3.7 Ga plate tectonics on the Earth; field evidence from

the Isua accretionary complex, West Greenland. J Geol 107:515–554
Krogh TE, Kamo SL, Kwok YY (2002) An isotope dilution, etch abrasion solution to the Akilia island U–Pb age controversy. Goldschmidt abstracts A419
Ludwig K (1997) Isoplot/Ex. Berkeley Geochronology Center, Publication 1
Martin H, Smithies RH, Rapp R, Moyen J-F, Champion D (2005) An overview of adakite, tonalite–trondhjemite–granodiorite (TTG), and sanukitoid: relationships and some implications for crustal evolution. Lithos 79:1–24
Maruyama S, Masuda T, Nohda S, Appel P, Otofuji Y, Miki M, Shibata T, Hagiya H (1992) The 3.9–3.8 Ga plate tectonics on the Earth: evidence from Isua, Greenland. Paper presented at the Evolving Earth Symposium, Tokyo Institute of Technol, Okazaki, Japan
McDonough WF and Sun SS (1995) The composition of the Earth. Chem Geol 120:223–253
McGregor VR (1973) The early Precambrian gneisses of the Godthåb district, West Greenland. Phil Trans R Soc Lond A 273:343–358
McGregor VR (1979) Archean gray gneisses and the origin of the continental crust: evidence from the Godthåb region, West Greenland. In: Barker F (ed), Trondhjemites, dacites and related rocks. Developments in Petrology. Elsevier, Amsterdam, vol 6, pp 169–204
McGregor VR (2000) Initial Pb of the Amîtsoq gneiss revisited: implications for the timing of early Archaean crustal evolution in West Greenland—comment. Chem Geol 166:301–308
McGregor VR, Friend CRL (1997) Field recognition of rocks totally retrogressed from granulite facies: an example from Archaean rocks in the Paamiut region, South-West Greenland. Precambrian Res 86:59–70
McGregor VR, Mason B (1977) Petrogenesis and geochemistry of metabasaltic and metasedimentary enclaves in the Amîtsoq gneisses, West Greenland. Am Mineral 62:887–904
McGregor VR, Friend CRL, Nutman AP (1991) The late Archaean mobile belt through Godthåbsfjord, southern West Greenland: a continent–continent collision zone? Bull Geol Soc Den 39:179–197
Mojzsis SJ, Harrison TM (2002) Establishment of a 3.83 Ga magmatic age for the Akilia tonalite (southern West Greenland). Earth Planet Sci Lett 202:563–576
Moorbath S, O'Nions RK, Pankhurst RJ, Gale NH, McGregor VR (1972) Further rubidium–strontium age determinations on the very early Precambrian rocks of the Godthåb district: West Greenland. Nature 240:78–82
Moorbath S, O'Nions RK, Pankhurst RJ (1973) Early Archaean age for the Isua iron formation, West Greenland. Nature 245:138–139
Moorbath S, Whitehouse MJ, Kamber BS (1997) Extreme Nd-isotope heterogeneity in the early Archaean—fact or fiction? Case histories from northern Canada and West Greenland. Chem Geol 135:213–231
Myers JS (1988) Early archaean Narryer Gneiss complex, Yilgarn Craton, Western Australia. Precamb Res 38:309–323
Nielsen SG, Baker JA, Krogstad EJ (2002) Petrogenesis of an early Archaean (3.4 Ga) norite dyke, Isua, West Greenland: evidence for early Archaean crustal recycling. Precamb Res 118:133–148
Nutman AP (1980) A field and laboratory study of the early Archaean rocks of northwest Buksefjorden, southern West Greenland. Unpublished PhD Thesis, University of Exeter, UK
Nutman AP (1990) New old rocks from Greenland. In: 7th international conference on geochronology, cosmochemistry and isotope geology. Geol Soc Aust Abstr, vol 27, pp 72
Nutman AP (2001) On the scarcity of >3900 Ma detrital zircons in ≤ 3500 Ma metasediments. Precamb Res 105:93–114
Nutman AP, Bridgwater D (1986) Early Archaean Amîtsoq tonalites and granites from the Isukasia area, southern West Greenland: development of the oldest-known sial. Contrib Mineral Petrol 94:137–148
Nutman AP, Collerson KD (1991) Very early Archean crustal-accretion complexes preserved in the North Atlantic Craton. Geology 19:791–794
Nutman AP, Bridgwater D, Fryer B (1984) The iron rich suite from the Amîtsoq gneisses of southern West Greenland: Early Archaean plutonic rocks of mixed crustal and mantle origin. Contrib Mineral Petrol 87:24–34
Nutman AP, Friend CRL, Kinny PD, McGregor VR (1993) Anatomy of an Early Archaean gneiss complex:3900 to 3600 Ma crustal evolution in southern West Greenland. Geology 21:415–418
Nutman AP, McGregor VR, Friend CRL, Bennett VC, Kinny PD (1996) The Itsaq Gneiss Complex of southern West Greenland; the world's most extensive record of early crustal evolution (3900–3600 Ma). Precamb Res 78:1–39
Nutman AP, Mojzsis, SJ, Friend CRL (1997a) Recognition of 3850 Ma water-lain sediments in West Greenland and their significance for the early Archaean Earth. Geochim Cosmochim Acta 61:2475–2484
Nutman AP, Bennett, VC, Friend CRL, Rosing MT (1997b) c. 3710 and ≤ 3790 Ma volcanic sequences in the Isua (Greenland) supracrustal belt; structural and Nd isotope implications. Chem Geol 141:271–287
Nutman AP, Bennett VC, Friend CRL, Norman MD (1999) Meta-igneous (non-gneissic) tonalites and quartz-diorites from an extensive ca. 3800 Ma terrain south of the Isua supracrustal belt, southern West Greenland: constraints on early crust formation. Contrib Mineral Petrol 137:364–388
Nutman AP, Friend CRL, Bennett VC, McGregor VR (2000) The early Archaean Itsaq Gneiss Complex of southern West Greenland: the importance of field observations in interpreting dates and isotopic data constraining early terrestrial evolution. Geochem Cosmochim Acta 64:3035–3060
Nutman AP, McGregor VR, Shiraishi K, Friend CRL, Bennett VC, Kinny PD (2002) ≤ 3850 Ma BIF and mafic inclusions in the early Archaean Itsaq Gneiss Complex around Akilia, southern West Greenland? The difficulties of precise dating of zircon-free protoliths in migmatites. Precamb Res 117:185–224
Nutman AP, Friend CRL, Bennett VC, McGregor VR (2004a) The Ameralik dykes of the Nuuk district, Greenland: multiple intrusion events starting from ca. 3510 Ma. J Geol Soc Lond 161:421–430
Nutman AP, Friend CRL, Barker SL, McGregor VR (2004b) Inventory and assessment of Palaeoarchaean gneiss terrains and detrital zircons in southern West Greenland. Precamb Res 135:281–314
O'Nions RK, Pankhurst RJ (1974) Rare-earth element distribution in Archaean gneisses and anorthosites, Godthåb area, West Greenland. Earth Planet Sci Lett 22:328–338
Patchett P J, Vervoort JD, Söderlund U, Salters VJM (2004) Lu–Hf and Sm–Nd isotopic systematics in chondrites and their constraints on the Lu–Hf properties of the Earth. Earth Planet Sci Lett 222:29–41
Polat A, Hofmann A, Rosing MT (2002) Boninite-like volcanic rocks in the 3.73.8 Ga Isua greenstone belt, West Greenland: geochemical evidence for intra-oceanic subduction zone processes in the early Earth. Chem Geol 184:231–254
Rosing M (1999) ^{13}C-depleted carbon microparticles in >3700 Ma seafloor sedimentary rocks from Greenland. Science 283:674–676
Schiøtte L, Compston W, Bridgwater D (1989) Ion probe U–Th–Pb zircon dating of polymetamorphic orthogneisses from northern Labrador, Canada. Can J Earth Sci 26:1533–1556

Smithies RH, Champion DC, Cassidy KF (1993) Formation of Earth's early continental crust. Precamb Res 127:89–101

Song B, Nutman AP, Liu D, Wu J (1996) 3800 to 2500 Ma crustal evolution in the Anshan area of the Lianing Province, northeastern China. Precamb Res 78:79–79

Tolstikhin I, Hofmann AW (2005) Primitive crust on the top of the metal magma ocean. Phys Earth Planet Inter 148:109–130

Vervoort JD, Patchett PJ, Gehrels GE, Nutman AP (1996) Constraints on early Earth differentiation from hafnium and neodymium isotopes. Nature 379:624–627

Watson EB (1996) Dissolution, growth and survival of zircons during crustal fusion: kinetic principles, geological models and implications for isotopic inheritance. Trans R Soc Edinb Earth Sci 87:43–56

Watson EB, Harrison TM (1983) Zircon saturation revisited: temperature and composition effects in a variety of crustal magma types. Earth Planet Sci Lett 64:295–304

White RV, Crowley JL, Myers JS (2000) Earth's oldest well-preserved mafic dyke swarms in the vicinity of the Isua greenstone belt, southern West Greenland (Geological Survey of Denmark and Greenland, Copenhagen). Geol Greenl Surv Bull 186:65–72

Whitehouse MJ, Kamber BS (2005) Assigning dates to thin gneissic veins in high-grade metamorphic terranes: a cautionary tale from Akilia, southwest Greenland. J Pet 46:291–318

Whitehouse MJ, Kamber BS, Moorbath S (1999) Age significance of U–Th–Pb zircon data from early Archaean rocks of west Greenland—a reassessment based on combined ion–microprobe and imaging studies. Chem Geol 160:201–224

Wyllie PJ, Wolf MB, van der Laan SR (1997) Conditions for formation of tonalites and trondhjemites: magmatic sources and products. In: De Wit M, Ashwal LD (eds) Greenstone belts. Oxford Science Publications, Oxford, pp 256–266

Yu Z, Norman M, Robinson P (2003) Major and trace element analysis of silicate rocks by XRF and laser ablation ICPMS using lithium borate fused glasses: matrix effects, instrument response, and results for international reference materials. Geostandards. Newsl J Geostand Geoanal 27:67–89